2016-11-01

Geochemical Comparison of Ancient and Modern Eolian Dune Foresets Using Principal Components Analysis

David A. Little
Brigham Young University

Geochemical Comparison of Ancient and Modern Eolian Dune Foresets

Using Principal Components Analysis

David A. Little

A thesis submitted to the faculty of
Brigham Young University
in partial fulfillment of the requirements for the degree of

Master of Science

Thomas H. Morris, Chair
Barry R. Bickmore
Jani Radebaugh

Department of Geological Sciences

Brigham Young University

ABSTRACT

Geochemical Comparison of Ancient and Modern Eolian Dune Foresets
Using Principal Components Analysis

David A. Little
Department of Geological Sciences, BYU
Master of Science

Geochemistry has been used to determine the provenance and diagenetic history of eolian sandstone deposits. However, the grain size, sorting, cementation, and detrital composition of eolian units can change along dune foreset laminae. The purpose of this study was to test for consistent trends of compositional change along dune foresets. Such trends could increase the quality of geochemical sampling of eolian sandstones and possibly aid in estimating the original height of ancient sand dunes. XRF data was gathered for both major and trace elements from the Pennsylvanian to Permian Weber Sandstone, Early Jurassic Navajo Sandstone, and modern Coral Pink Sand Dunes of southern Utah. Data was plotted using both 2-dimensional scatter plots and 3-dimensional principal components analysis (PCA) plots. The PCA plots proved to be the most informative and suggest that there are no consistent, statistically significant geochemical trends within or between the three units sampled. However, this study found that PCA was able to show significant geochemical differences between the three units sampled, even when they are all dominated by a single mineral (>90% quartz). The Weber Sandstone had the most varied composition, and dunes within the unit could be highly dissimilar to each other. The Navajo Sandstone had less overall geochemical variability than the Weber Sandstone, and individual dunes were similar to each other. The modern Coral Pink Sand Dunes had much less compositional variation than either of the other two units, and dunes in this unit were very similar to each other.

Keywords: Weber Sandstone, Navajo Sandstone, Coral Pink Sand Dunes, principal components analysis, XRF, geochemistry, eolian

ACKNOWLEDGMENTS

I would like to thank my advisor, Tom Morris, as well as my other committee members, Barry Bickmore and Jani Radebaugh, for their extraordinary patience in working with me and helping me complete this project. A special thanks goes to Dr. Bickmore for his help in teaching me so much about statistics and helping me understand my data. I would also like to thank Dave Tingey and David Tomlinson and the others who work or have worked in the BYU XRF laboratory for their assistance. I am grateful for the huge amounts of help I received on this project from my field and lab assistants, my minions of science, Chanse Rinderknecht, Trevor Tuttle, and Josh Whitmer. Finally, I need to thank my wife for her invaluable support and encouragement over the years I worked to get this done.

TABLE OF CONTENTS

LIST OF TABLES

LIST OF FIGURES

INTRODUCTION

Geochemistry of eolian dunes has been used for multiple purposes, including provenance determination (Link et al., 2014), diagenetic analysis (Beitler et al., 2005), and distinguishing between eolian units of similar appearance (Phillips and Morris, 2012). The purpose of this study was to test the hypothesis that geochemical trends exist along foreset laminae of eolian dunes within and between several units of different age. If these trends proved consistent, they could significantly improve the quality of geochemical sampling in eolian units and aid in predicting the degree of paleodune preservation.

To test this, 197 samples were taken from 18 modern and ancient sand dunes, 6 dunes each from the Pennsylvanian/Permian Weber Sandstone, Early Jurassic Navajo Sandstone, and the modern Coral Pink Sand Dunes. Dunes of various size (i.e. different foreset lengths) were sampled to determine if there were differences in geochemical trends between large and small dunes. If certain trends were detected, this might assist in estimating the original height of paleodunes.

Units of Study

The state of Utah contains abundant exposures of eolian sandstones of different age (termed units in this study). Samples for this study were collected from well-exposed outcrops of the Pennsylvanian/Permian Weber Sandstone of northeastern Utah and the Early Jurassic Navajo Sandstone of northeastern and central Utah. The Coral Pink Sand Dunes, a modern dune field in southern Utah, also provided exceptional exposures (Figure 1).

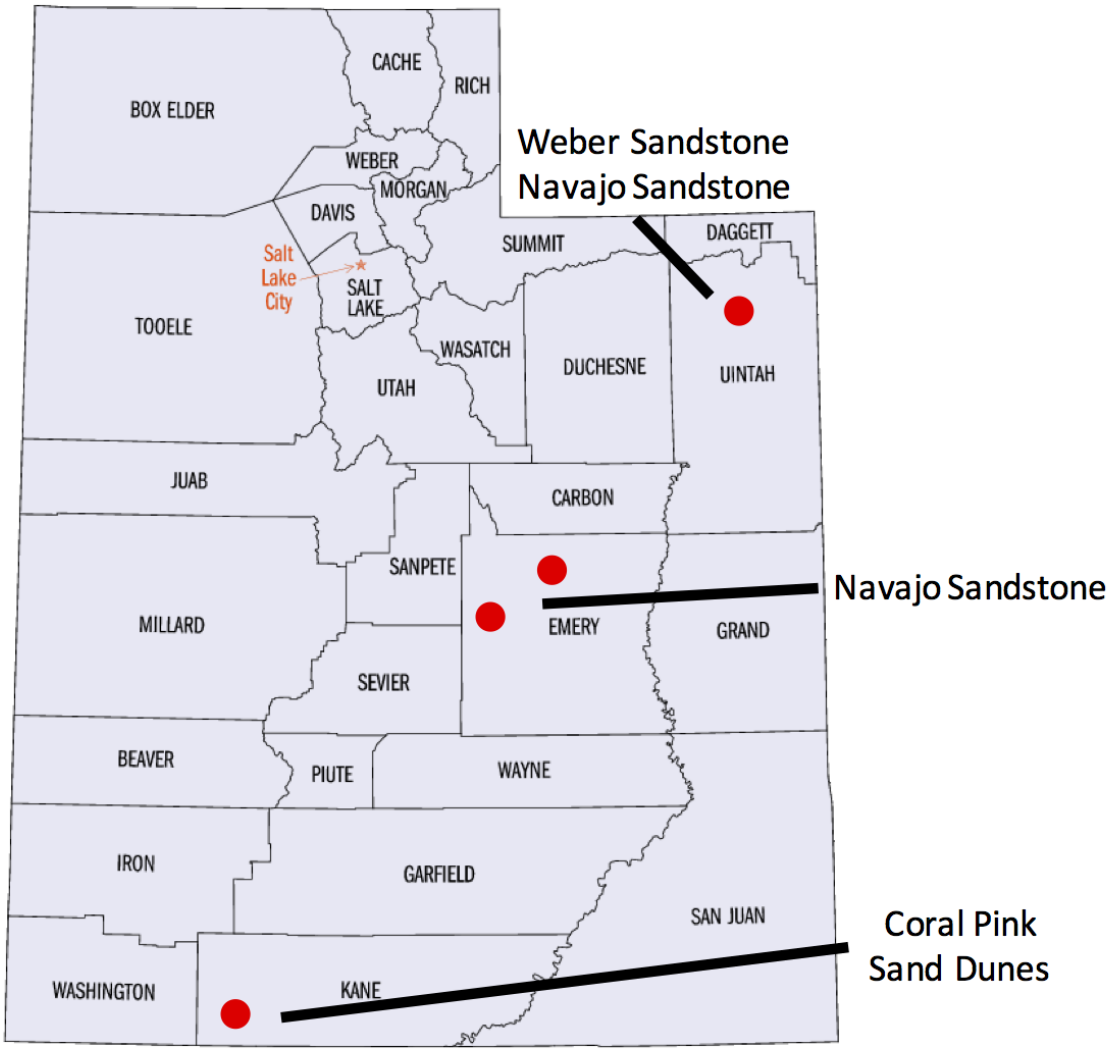

Figure 1. Locations of sampled units. Eolian portions of the Weber Sandstone were sampled near Vernal, Utah. The Navajo Sandstone was sampled from dunes near Vernal, Utah and from parts of the San Rafael Swell. Modern Coral Pink Sand Dunes were sampled in southern Utah near Coral Pink Sand Dunes State Park.

The Weber Sandstone is a primarily eolian sandstone with some shallow marine and fluvial components that was deposited from the Middle Pennsylvanian through the early Permian (Depret, 2005; Adams, 2006; Link et al., 2014). It is present in northern Utah, northwestern Colorado, and southwestern Wyoming (Adams, 2006). Eolian environments were intermittently present in this area from the late Paleozoic through the Jurassic. The source of sand for the

Weber Sandstone is mostly from the Yavapai-Mazatzal provinces of Colorado with some lesser amount of grains sourced from the Grenville Province in eastern North America (Link et al., 2014). At its eastern edge, the eolian part of the Weber Sandstone intertongues with marine and fluvial units due to a complex interplay between deposition and tectonics (Bissell, 1964; Crowell, 1978; Fryberger, 1979). The eolian portion of the Weber Sandstone is composed of a fine- to very fine-grained, sub-angular to sub-rounded, sub-arkosic sandstone. It contains large-scale cross-bedding (Depret, 2005; Adams, 2006). The color can be gray, brown, white, or light red (Depret, 2005).

The Navajo Sandstone is an eolian sandstone that was deposited in the Early Jurassic as part of a massive erg that extended over much of the Colorado Plateau in what is now the western United States (Blakey, 1988; Beitler et al., 2005). The Navajo Sandstone correlates with both the Nugget Sandstone in the northern Colorado Plateau, and the Aztec Sandstone to the southwest (Hintze and Kowallis, 2009). The Navajo Sandstone can be hundreds of meters thick (Blakey, 1988; Dalrymple and Morris, 2007, Hintze and Kowallis, 2009). The sediment for the Navajo Sandstone was derived primarily from the Appalachian Mountains of eastern North America (Dickinson and Gehrels, 2003; Rahl et al., 2003; Campbell et al., 2005). The Navajo Sandstone is a fine- to medium-grained subfeldspathic to quartz arenite (Chan et al., 2000; Dalrymple and Morris, 2007).

The Coral Pink Sand Dunes are active eolian dunes in southwestern Kane County, Utah. The Coral Pink sands include a variety of migrating and stabilized dune types, including transverse, barchanoid, star, parabolic, and vegetated linear dunes (Ford and Gillman, 2000). The sand grains that comprise the dunes are 98% SiO_2 and are named after the coral pink color caused by iron oxide staining on grain surfaces. The dunes lie in the transition zone between the

Great Basin section of the Basin and Range Province and the Colorado Plateau. The dunes are accumulating along a bedrock escarpment of the Sevier Fault. Wind accelerates through breaks in the southward-flanking Vermillion Cliffs and then decelerates upon entering the catchment basin along the Sevier Fault at Coral Pink Sand Dunes. The chronology and evolution of the Coral Pink Sand Dunes are not well known, though they are thought to be sourced from the Navajo Sandstone, which is exposed next to the dunes, and directly underlies the dunes in places. Other units that may have contributed grains to the Coral Pink Sand Dunes include the Page Sandstone and Entrada Sandstone (Ford and Gillman, 2000).

Methods

For each dune, the length of the foreset was measured, and ten equally spaced points sampled (Figure 2). In a few places, more than one sample was taken to be used to determine compositional consistency. Each sample was tested for both major and trace element concentration using XRF analysis. XRF data can be found in Appendix A.

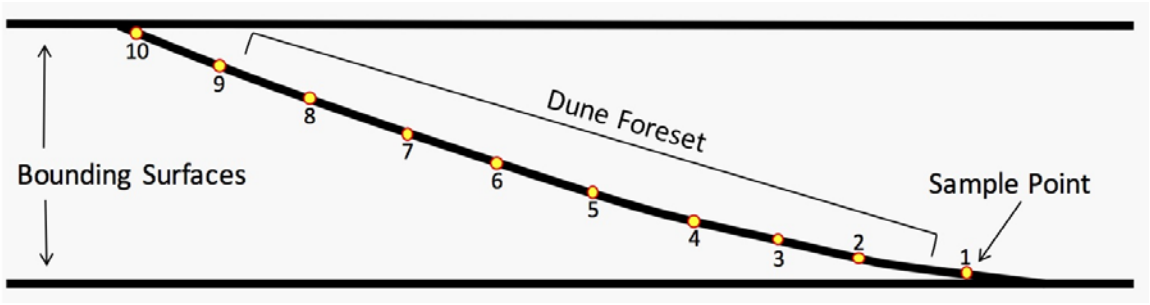

Figure 2. Illustration of the locations of sample points along a dune foreset. Foresets were measured and sampled at ten equally-spaced points. For paleodunes, the foreset length was measured between bounding surfaces. For modern dunes, the foreset was measured from toe to crest.

XRF data was plotted against foreset length to look for geochemical trends in the dunes sampled. Principal components analysis (PCA) was then employed to better illustrate

geochemical data when comparing different units and the dunes within different units (McKillup and Dyar, 2010).

Sample Collection

For each of the three units, six dunes of various sizes were sampled (termed small, medium, and large), with ten equally-spaced samples taken from each dune. The spacing between samples varied between dunes due to differences in foreset length. Dune designations and foreset lengths are given in (Table 1).

Names and Foreset Lengths of Sampled Dunes		
Unit Sampled	Dune Name	Foreset Length (inches)
Weber Sandstone	Weber S1	189
	Weber S2	189
	Weber M1	288
	Weber M2	490.5
	Weber M3	379.8
	Weber L1	1044
Navajo Sandstone	Navajo S1	191.7
	Navajo S2	217.8
	Navajo M1	684
	Navajo M2	742.5
	Navajo L1	1944
	Navajo L2	1436.4
Coral Pink Sand Dunes	Coral Pink S1	108
	Coral Pink S2	504
	Coral Pink M1	765
	Coral Pink M2	846
	Coral Pink L1	1881
	Coral Pink L2	1440

Table 1. This table contains the names given to and foreset lengths of sampled dunes. The letters "S", "M", and "L" in the dune names stand for "small", "medium", and "large" dunes, respectively. Those descriptors are used to describe subjective, relative sizes of dunes to other dunes in the same unit.

Paleodunes were sampled if both upper and lower bounding surfaces were visible and when they were exposed in as close to a longitudinal cross-section as possible. A single foreset for each dune was selected for sampling and measured for length. A foreset in a paleodune, for the sake of this study, was identified by following a single grainflow lamination from the base of the dune upwards towards the upper bounding surface. If the grainflow lamination terminated higher up the dune, the grainfall or grainflow lamination into which the initial lamination terminated was followed to the upper bounding surface (Hunter 1977, Figure 3).

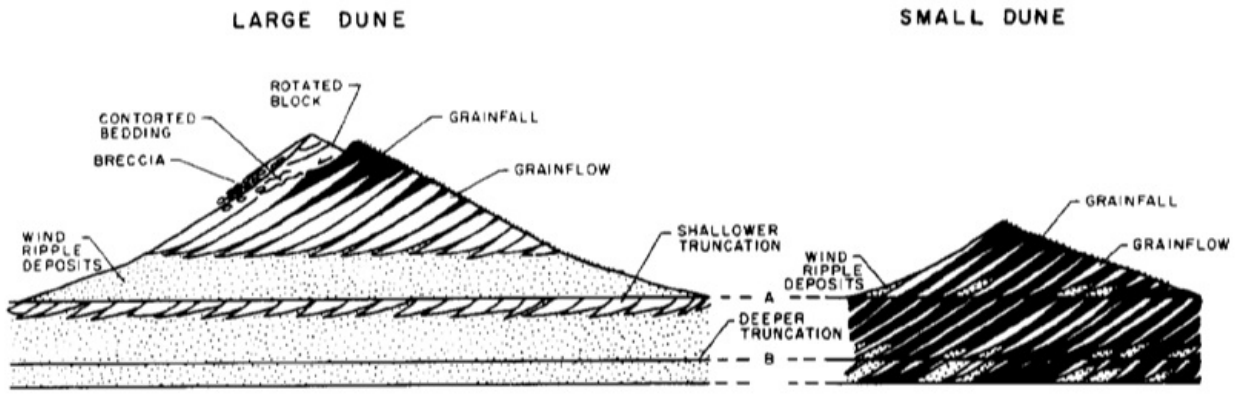

Figure 3. Idealized dune cross-sections show the relationships between grainflow and grainfall laminae. They can, at times, terminate into each other. From Kocurek and Dott (1981).

Ten equally-spaced points were marked along the foreset and sampled. Lithified dunes of the Weber Sandstone and Navajo Sandstone were sampled using a 1-inch diameter core plug drill. Because the core plug drill used to collect samples was one inch in diameter, most samples included several different laminae, both grainflow and grainfall (Figure 4). Samples from the Coral Pink Sand Dunes were collected along gain flow laminae by scooping grains into plastic vials. A few points were sampled more than once to determine consistency of XRF results,

which can be seen in the XRF data in Appendix A. Repeat samples were similar to each other when analyzed with PCA. In total, 197 samples were taken from 18 dunes across the three units.

Figure 4. An example of a sample from the Weber S2 dune extracted using a 1-inch diameter core plug drill. Note that even with just a 1-inch diameter core, several different laminae were sampled. Whenever possible, the portion of the plug farthest from the exposed surface was used for XRF analysis to avoid surface effects. The approximate portion of this plug used is shown in the red box.

XRF Analysis

All samples were prepared for XRF analysis using the standard procedures of the Brigham Young University Geological Sciences XRF Laboratory. Analysis was done with a Rigaku ZSX Primus II XRF for both major and trace element concentrations. Major elements tested for were SiO_2, TiO_2, Al_2O_3, Fe_2O_3, MnO, Mgo, CaO, Na_2O, K_2O, and P_2O_5. Trace

elements tested for were Ba, Ce, Cr, Cu, Ga, La, Nb, Nd, Ni, Pb, Rb, Sc, Sm, Sr, Th, U, V, Y, Zn, and Zr. Data from XRF analysis can be found in Appendix A.

GEOCHEMICAL DATA ANALYSIS RESULTS

Geochemical Data Analysis

After XRF analysis was performed on all collected samples, the data were plotted and analyzed to determine if there were any consistent changes in geochemistry along foresets within and between the three units. XRF data points were plotted against both their distance and relative position along a foreset. Review of 720 plots of such combinations of the data revealed no statistically significant trend in geochemical change along eolian dune foresets within individual dunes, within units as a whole, or between different units.

Appendix B contains a table that shows the trends of changes in element concentrations for each dune sampled. Most trends were not consistent within or between sampled units. Even when a trend of a given element was consistent within a formation, the trend was deemed not statistically significant due to the large spread in the data (Eggett, personal communication, 2015). Two examples will be shown from elements and dunes that appeared to have promising trends, but ended up not being statistically significant.

Figure 5 shows an example of one of these trends from the Coral Pink Sand Dunes. While a trend line of Fe_2O_3 weight percent in each sampled dune from the Coral Pink Sand Dunes shows Fe_2O_3 increasing in concentration upwards along the foreset, the spread in the data means the trend lines are weak. With all of the dunes plotted together, no overall pattern of Fe_2O_3 concentration as it relates to distance along foresets was identified. Even when an element

showed consistent but statistically weak trends within each sampled dune of a unit for a certain element, that element did not show the same trends in the other units.

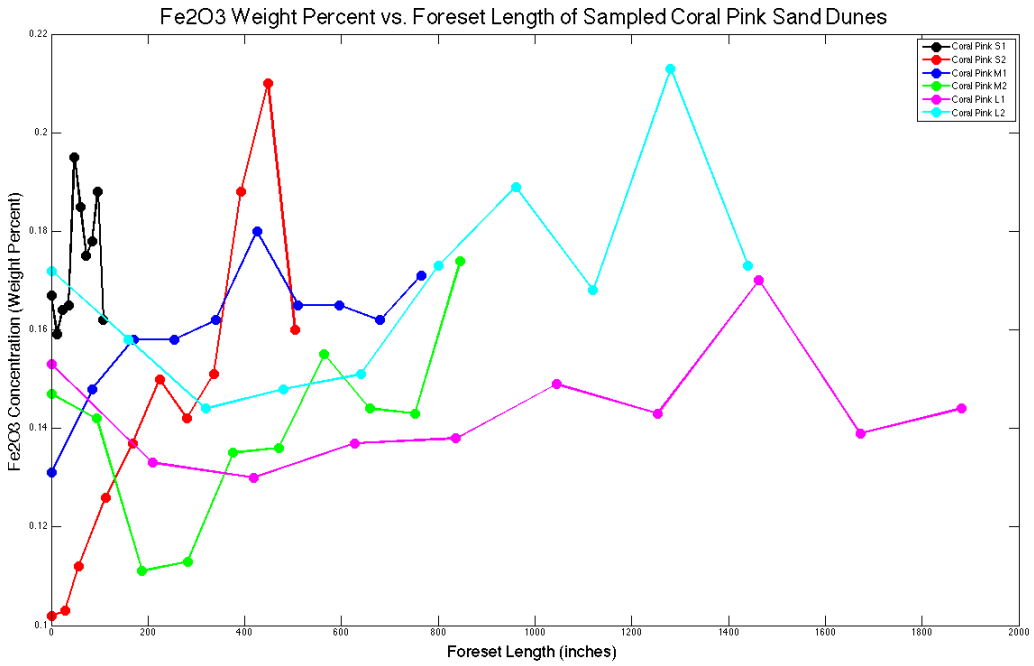

Figure 5. This plot shows Fe_2O_3 concentrations verses distance along foreset for all sampled Coral Pink Sand Dunes. Every individual sampled dune in this unit showed Fe_2O_3 concentrations increasing upwards from the toe of the dune, but there was no consistent, statistically significant trend when data was looked at collectively.

For some elements, such as Cu from the Navajo Sandstone, plotting the concentration of all samples from a single unit together seemed to have an upper boundary of concentration that decreased with distance upward along a foreset (Figure 6). In these cases, the trends of that element's concentration within the unit's individual dunes was not consistent (i.e. Cu concentration increased upwards along the foreset in some Navajo Sandstone dunes, and decreased in concentration upwards along the foreset in others). However, many of the high element concentration values at low foreset lengths were due to a low number of samples. In

addition, there were few values at high foreset length values, as not all dunes had the same lengths of foresets. The statistical value of such overall trends was deemed too weak to be useful (Eggett, personal communication, 2015), and was not found in the other units for the same element.

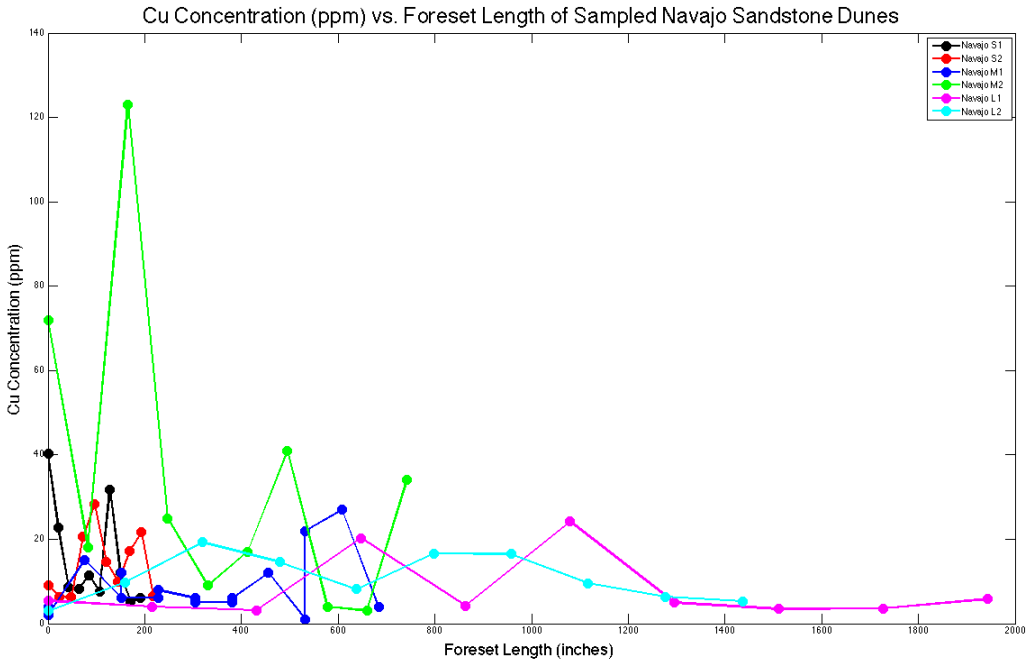

Figure 6. This is a plot of Cu concentrations verses foreset lengths for all sampled dunes in the Navajo Sandstone. An overall pattern appears to be present, but there is no consistency to the trend in individual dunes.

Principal Components Analysis

After 2-dimensional plotting of XRF data against sample position and distance along dune foresets failed to uncover any statistically significant trends in geochemical change, principal components analysis (PCA) was employed. PCA can be used to better understand data distribution with a large number of variables. PCA utilizes linear correlations between *n* variables, rotating the *n*-dimensional axes to create new variables (principal components) that are

linear combinations of the original variables, so as to pack the greatest fraction of the variance into the fewest variables. A smaller number of the new variables can then be used to describe the dataset in a more understandable manner without losing as much information about the data. It has been suggested that enough principal components should be used to explain at least 70% of variance (McKillup and Dyar, 2010).

For all three units, PCA was done on; 1 – all elements, 2 – major elements only, and 3 – trace elements only. In each case, it was found that three principal components are required to describe at least 70% of the data.

Logarithms of the data were not used before performing PCA because of the presence of multiple valid zero values for the concentration of some elements and limited skewness in the data. Substituting very small values for zeros to perform PCA before taking the logarithm of the data didn't substantially change the relationships between dunes or units, and so this step was deemed unnecessary.

No log of the data was used before performing PCA because of the presence of multiple valid zero values for the concentration of some elements and a lack of major skewness in the data. Substituting very small values for zeros to perform PCA on a log of the data didn't substantially change the relationships between dunes or units, and so this step was deemed unnecessary.

PCA of All Elements

When PCA was used on all elements together (SiO_2, TiO_2, Al_2O_3, Fe_2O_3, MnO, Mgo, CaO, Na_2O, K_2O, P_2O_5, Ba, Ce, Cr, Cu, Ga, La, Nb, Nd, Ni, Pb, Rb, Sc, Sm, Sr, Th, U, V, Y, Zn, and Zr), it was found that the first three principal components describe 70.9% of the data –

48.8% from the first, 12.2% from the second, and 9.9% from the third. Appendix C shows plots of geochemical data in two dimensions using only the first two principal components. If compared with three-dimensional plots using the first three principal components, which are shown below, the importance of using the third principal component to better understand data distribution can clearly be visualized.

Table 2 shows the load contribution of each element to these first three principal components. Nearly all of the elements tested for, all but MgO and Na_2O, contributed significantly to one of the first three principal components. With so many significant contributors to the first three principal components, it is difficult to identify specific sedimentary or diagenetic processes causing the distribution of the data.

Contributions of All Elements to First Three Principle Components			
Element	**PCA 1 Contribution**	**PCA 2 Contribution**	**PCA 3 Contribution**
SiO2	-0.1864	-0.3206	-0.1124
TiO2	0.2472	0.0007	-0.0226
Al2O3	0.2378	-0.0625	-0.0854
Fe2O3	0.1887	-0.0185	0.0969
MnO	0.1272	0.0893	0.2667
MgO	0.1008	0.2177	0.1393
CaO	0.0280	0.4701	0.1617
Na2O	0.0371	-0.0602	-0.0058
K2O	0.2094	-0.1061	-0.1286
P2O5	0.2284	-0.0469	0.0226
Ba	0.1135	-0.0735	0.0015
Ce	0.2412	0.0173	-0.0450
Cr	0.0038	-0.2085	0.4789
Cu	0.0258	-0.1883	0.4648
Ga	0.2378	-0.0744	-0.0751
La	0.2341	-0.0019	-0.0177
Nb	0.2443	-0.0247	-0.0258
Nd	0.1517	-0.3380	-0.0702
Ni	-0.0061	-0.2047	0.5007
Pb	0.2144	-0.0342	-0.0629
Rb	0.2048	-0.1087	-0.1224
Sc	0.1309	0.3483	0.1483
Sm	0.0689	-0.4217	-0.1052
Sr	0.1755	-0.0249	-0.0704
Th	0.2298	0.0444	-0.0236
U	0.2181	0.1101	-0.0015
V	0.2349	0.0181	0.0505
Y	0.2524	0.0247	0.0016
Zn	0.1242	-0.1278	0.2573
Zr	0.2153	0.0919	-0.0220

Table 2. This table shows all elements for which concentrations were measured using XRF data, and their relative contributions, or loadings, to the first three principal components. Higher positive or negative values indicate higher positive or negative correlation, respectively, within that calculated principal component. If the absolute value of an element's contribution to a principal component was within a factor of two of the highest contributor, it was deemed significant. Significant contributors are highlighted in green. Most elements significantly contributed to the first principal component, and all but MgO and Na_2O contributed significantly to at least one of the first three principal components.

When the first three principal components of all elements from all three units sampled are displayed on a 3-dimensional scatter plot (Figure 7), some comparisons can be made relating to their composition. The Weber Sandstone is the most compositionally varied of the three units sampled, and the active Coral Pink Sand Dunes are the least varied. Weber Sandstone data are split into three converging branches. Navajo Sandstone data is concentrated along one of these branches, and all Coral Pink Sand Dunes data is relatively tightly concentrated where the three branches of Weber Sandstone and Navajo Sandstone data converge.

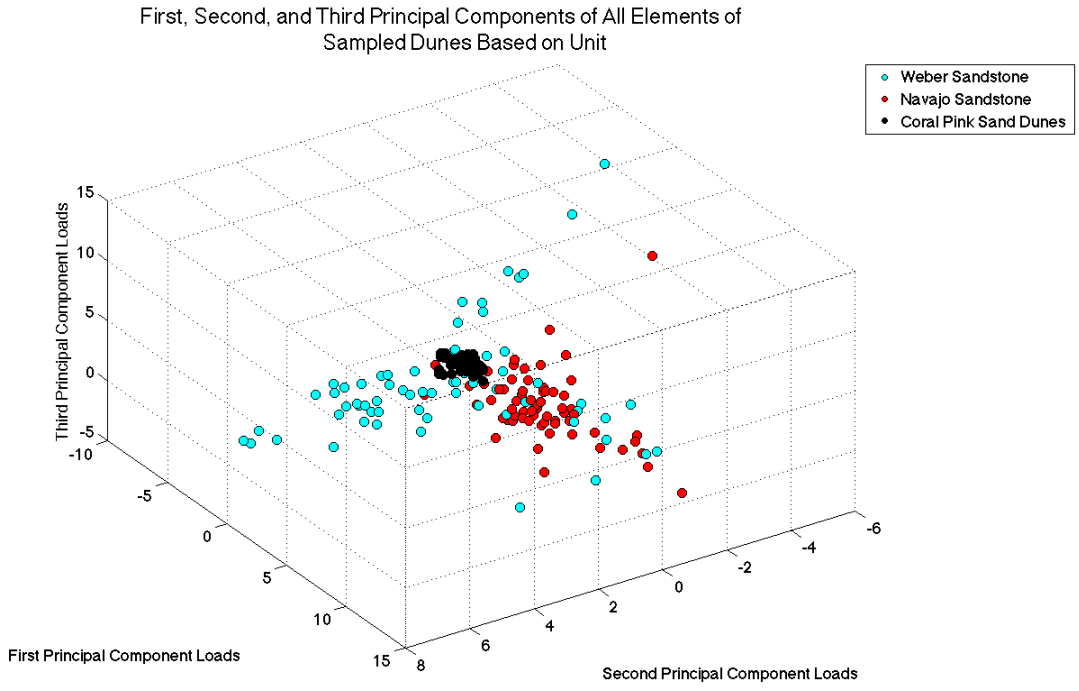

Figure 7. This is a plot of the first three principal components of all elements for all units sampled. The three different units are separated by color. The Weber Sandstone (in blue) is the most varied of the three units, with samples forming three branches. The Navajo Sandstone is less spread than the Weber Sandstone, but is concentrated around one of the three branches containing samples from the Weber Sandstone. Samples from the Coral Pink Sand Dunes are concentrated where the three branches converge, and have far less spread than either of the two units containing paleodunes.

Additional information was gained when the first three principal components were displayed by unit and individual dunes could be more clearly displayed. For example, the data from the first three principal components of Weber Sandstone data show the same three distinct branches that appear from the combined data of all three units (Figure 8). One of the branches is comprised of data entirely from one dune, and another is largely formed from data of a second dune. The other four dunes sampled from the Weber Sandstone are mostly contained in the third branch. The regions where data from each of these four dunes of the third branch are plotted have significant overlap, showing that these dunes are compositionally similar to each other. All three branches converge, and every dune sampled has some points at or near the area of convergence. With one exception, the Weber M1 dune, the data from dunes were well grouped by dune.

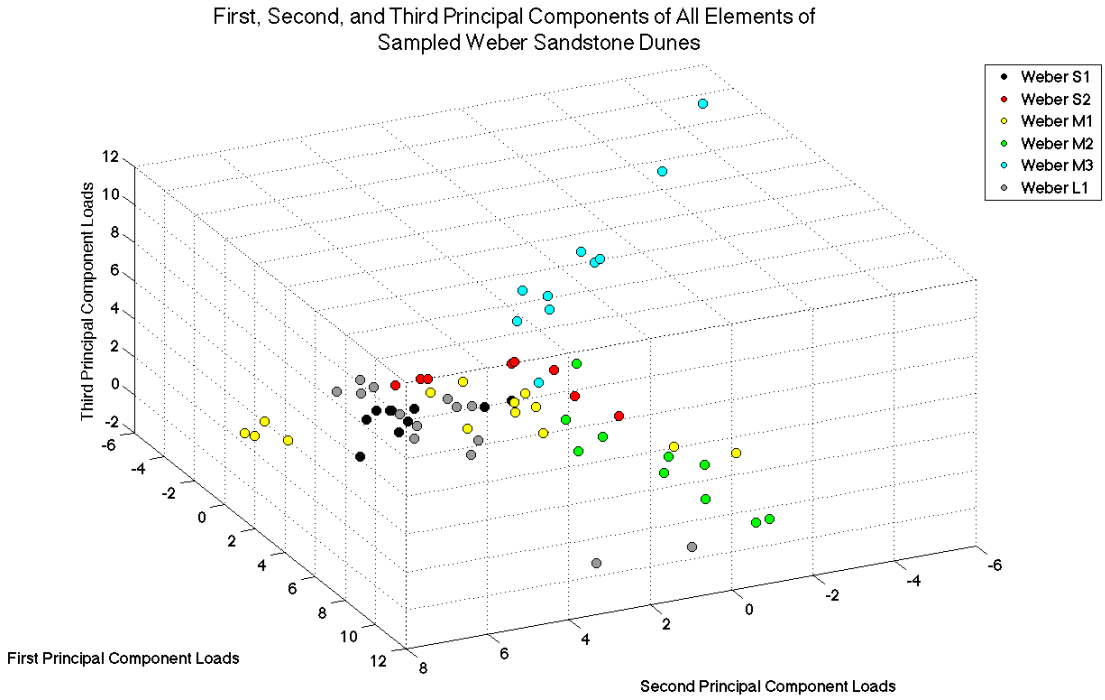

Figure 8. Plot of the first three principal components of Weber Sandstone samples, colored by dune. The same three branches that appeared when all dunes were plotted together are still present. One branch is

comprised entirely of the Weber M3 dune, and one largely from the Weber M2 dune. Dunes plotting apart from each other indicates that Weber Sandstone dunes can be highly dissimilar to each other compositionally.

Plots of the first three principal components of sampled Weber Sandstone dunes showed that the length of a dune foreset did not control compositional variation of dunes. Dunes with shorter foresets showed about as much compositional variability as those with longer foresets. In addition, when sample position along a foreset (see figure 2) was considered together with principal component plots, no consistent pattern was observed. An example of sample position data plotted together with the principal components of geochemical data of Weber Sandstone dune Weber M3 is given in Figure 9. None of the dunes from any of the sampled units showed consistent patterns when plotted using principal components by either sample position or distance along foreset.

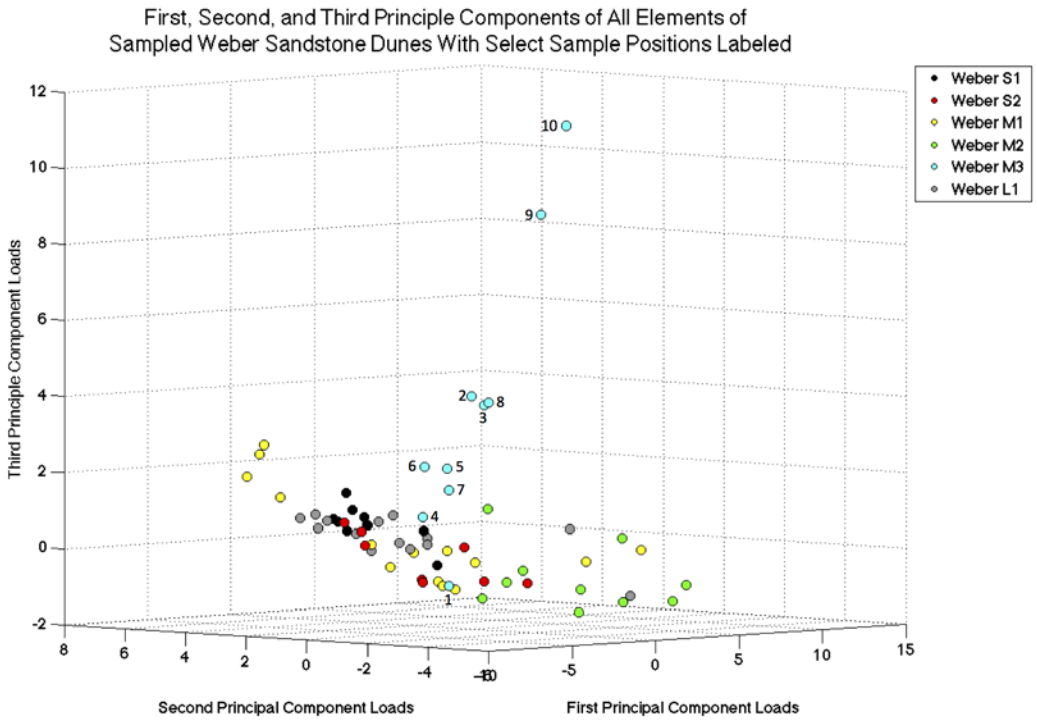

Figure 9. This plot contains the same data as Figure 8, but is oriented to better show the Weber M3 dune (shown in blue). Sample position numbers (see Figure 2) have been displayed to show the lack of any consistent pattern between sample position and composition. The relationship between differences in composition as shown through PCA and sample position was different for each dune, showing the lack of any overall trends. So even if there appears to be a pattern (such as samples from positions 8, 9, and 10 appearing sequentially in the Weber M3) in parts of a dune, the other dunes had samples plot in a different order in their relative branches.

When plotted together with the Weber Sandstone, data from the Navajo Sandstone was concentrated along one of the three branches. Plotted alone and broken out by dune in Figure 10, Navajo Sandstone data show that, unlike in the Weber Sandstone, regions containing data from each of the six sampled dunes overlap with other Navajo Sandstone dunes. There was also less significant spread in the data relative to the Weber Sandstone.

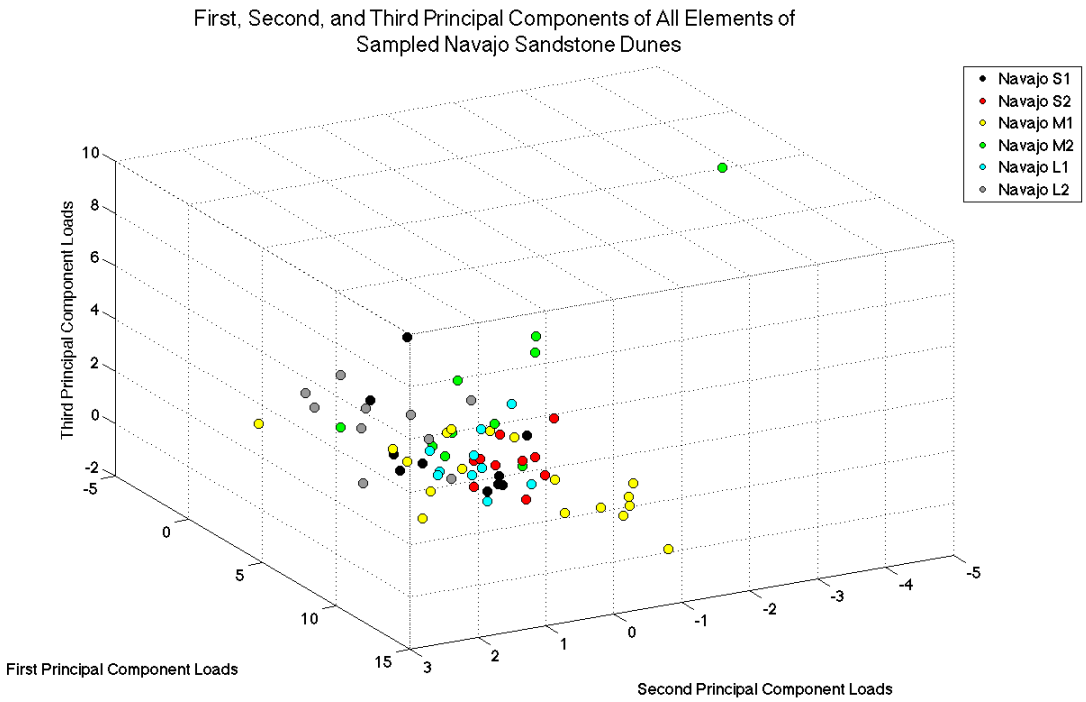

Figure 10. Plot of the first three principal components for all element data from the Navajo Sandstone, colored by dune. Note that all of the dunes overlap with other Navajo Sandstone dunes, indicating a high degree of compositional similarity.

Interestingly, the data collected from all six of the Coral Pink Sand Dunes had, as a whole, less spread than most individual dunes from either the Weber Sandstone or the Navajo Sandstone. Like the Navajo Sandstone, all of the data from the dunes of the Coral Pink Sand Dunes had a great deal of overlap with each other (Figure 11).

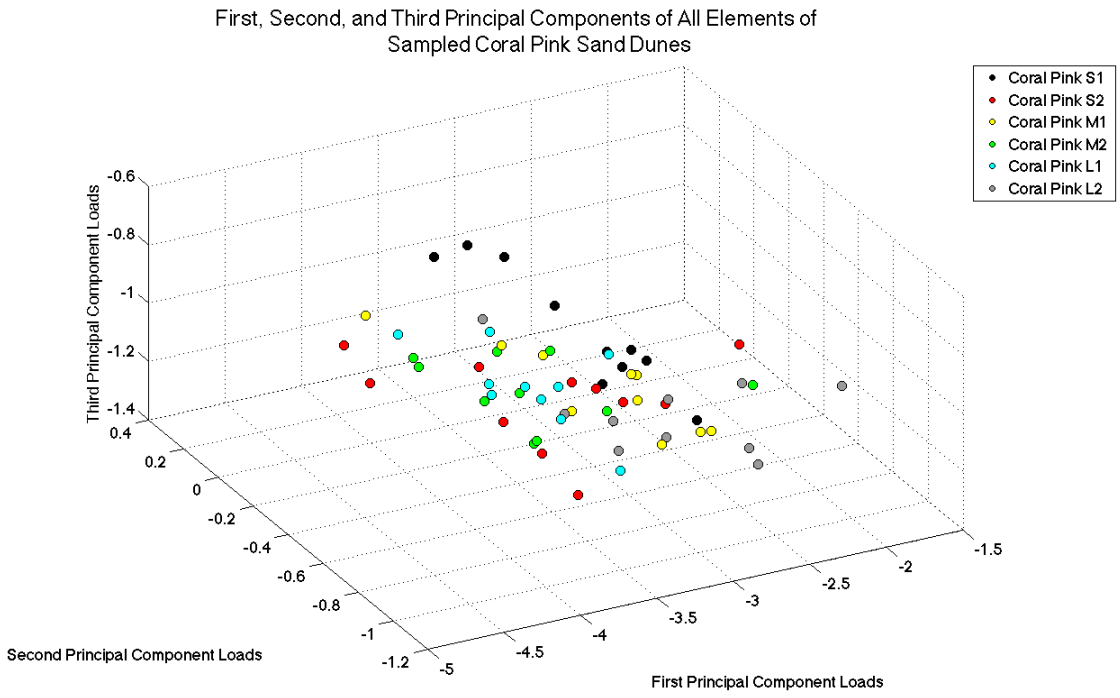

Figure 11. Plot of the first three principal components of all elements from the Coral Pink Sand Dunes, colored by dune. As with the Navajo Sandstone, every dune overlaps with others, showing they are compositionally similar. Note that the scale of the axes makes the data look more spread out than it really is. See Figure 7 to compare the spread of the different units to each other.

PCA of Major Elements

When PCA was performed using only the major elements (SiO_2, TiO_2, Al_2O_3, Fe_2O_3, MnO, Mgo, CaO, Na_2O, K_2O, and P_2O_5), the first three principal components described 80.2% of the data – 49.5% from the first principal component, 18.0% from the second, and 12.7% from the third. Every major element significantly contributed to at least one of the first three principal components, with only CaO and Na_2O not significantly contributing to the first principal component (Table 3).

Contributions of Major Elements to First Three Principle Components			
Element	**PCA 1 Contribution**	**PCA 2 Contribution**	**PCA 3 Contribution**
SiO2	-0.3658	-0.3669	-0.0189
TiO2	0.3924	-0.1113	-0.0192
Al2O3	0.3966	-0.2555	-0.1656
Fe2O3	0.3386	-0.0474	0.4657
MnO	0.2846	0.2500	-0.0810
MgO	0.2306	0.3736	-0.0969
CaO	0.1025	0.6534	0.0703
Na2O	0.0698	-0.1253	0.8263
K2O	0.3558	-0.3325	-0.2068
P2O5	0.4052	-0.1736	-0.0920

Table 3. Major elements analyzed and relative contributions to the first three principal components. Elements with a significant contribution to a principal component are highlighted in green. Every major element contributed significantly to at least one of the first three principal components, and all but CaO and Na_2O contributed significantly to the first principal component.

When data of the first three principal components of major elements from the three units are plotted together (Figure 12), there are some notable differences from the all elements plot. One of the three main branches of Weber Sandstone data is gone, and both Navajo Sandstone and Coral Pink Sand Dunes data have a higher relative amount of spread.

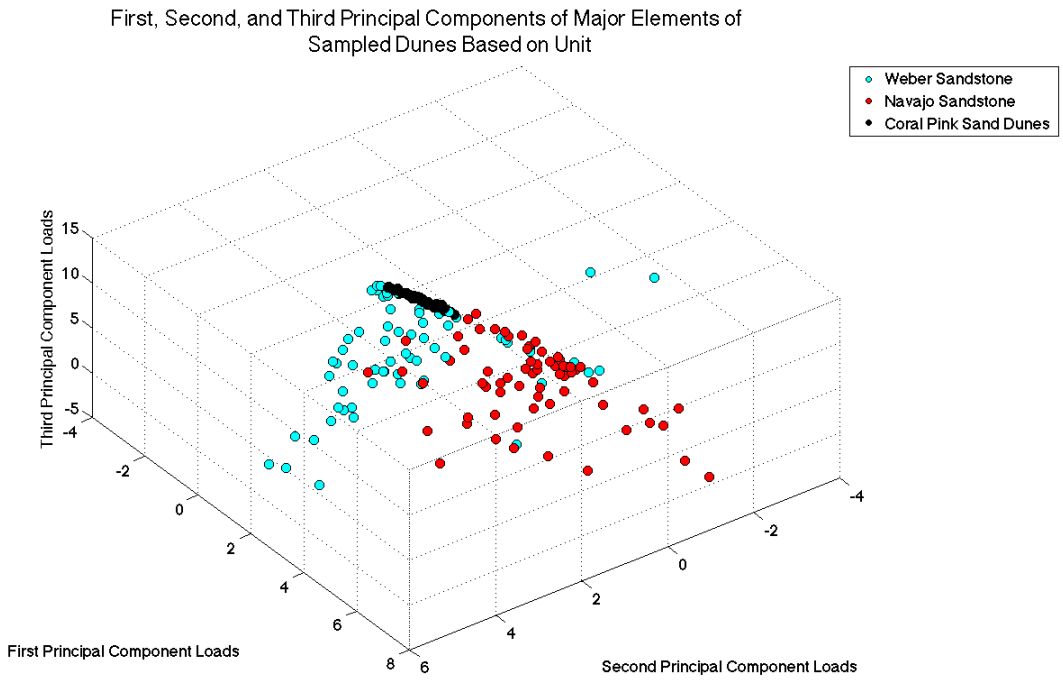

Figure 12. Plot of the first three principal components of major elements for all units. Compared to Figure 7, one of the three branches of Weber Sandstone data is missing. The major element data from this dune is located in a tight group where the two remaining branches converge. The two data points in the upper right of the figure are not remnants of the missing branch, but are from a different dune. This can be seen more easily in Figure 13, when only Weber Sandstone dunes are plotted.

When the first three principal components of major element data were plotted by unit (Figures 13, 14, and 15), the most significant difference from when all elements were plotted together was from the Weber Sandstone. One of the three branches from the plot of all element data is missing, and the dune that comprised that branch, Weber M3, instead plotted very tightly in the area where the branches converge along with the data from the Coral Pink Sand Dunes (Compare Figures 8 and 13).

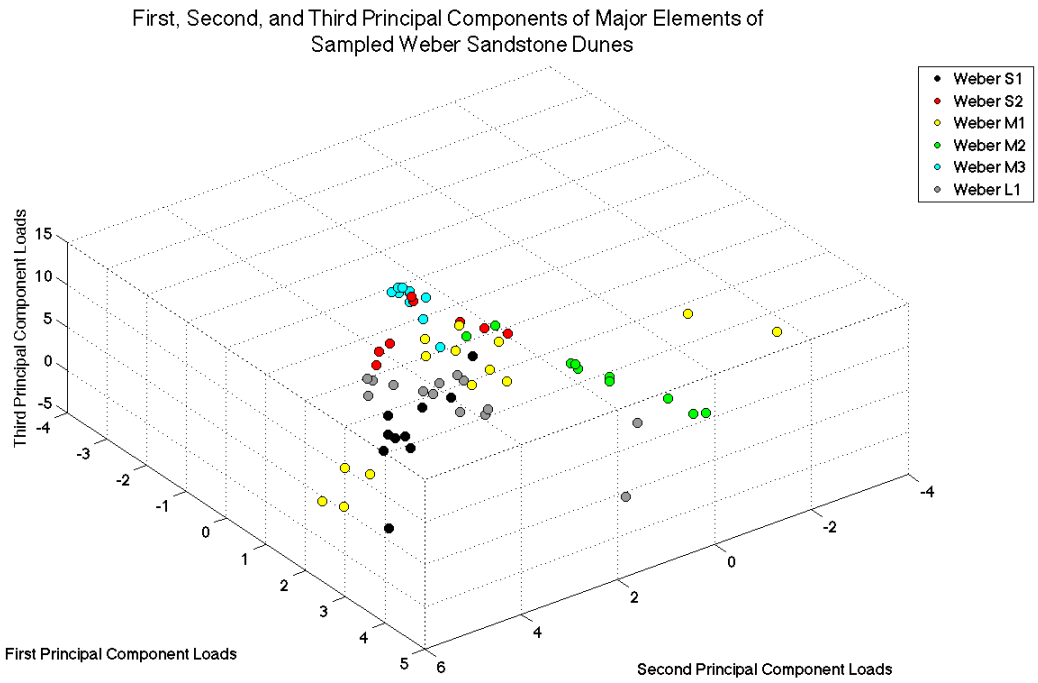

Figure 13. Plot of the first three principal components of major element data from the Weber Sandstone. Note that the Weber M3 dune, plotted in blue, no longer comprises a third branch in the data as it did when all elements were used for PCA (see Figure 8). This is the only dune that had a major change in distribution pattern when a different dataset of elements was used. Further geochemical studies in the Weber Sandstone may need to take this into account. Dunes in the Weber Sandstone still have much less overlap with each other than in the other units, indicating that they can have a high degree of compositional dissimilarity.

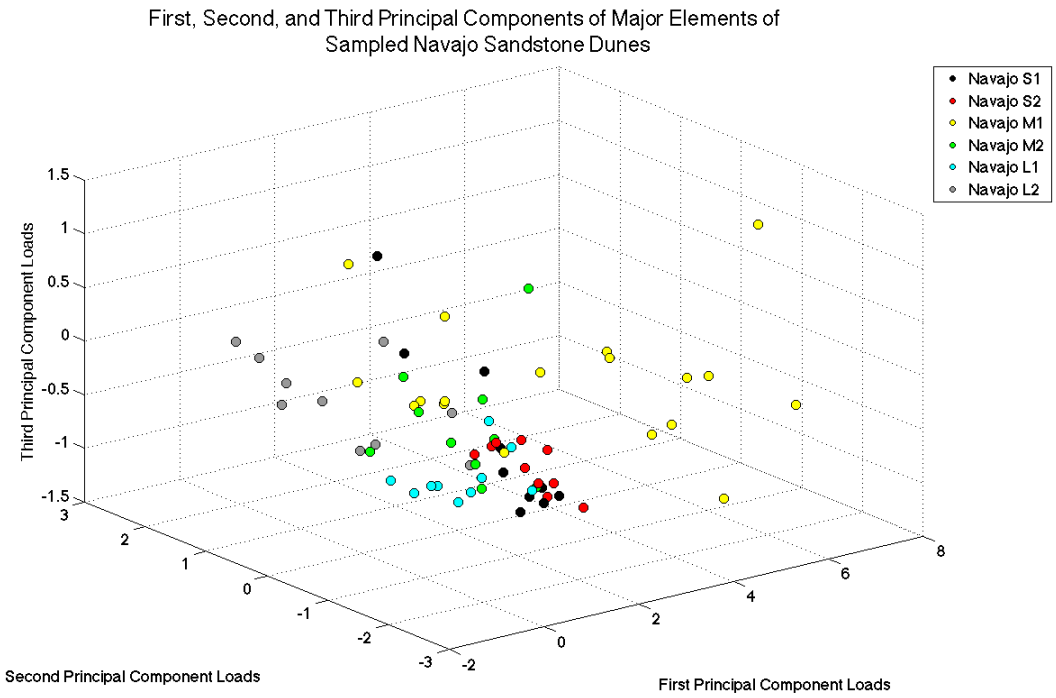

Figure 14. Plot of the first three principal components of major element data from the Navajo Sandstone. Note that all dunes have some overlap with other dunes, indicating a high degree of similarity.

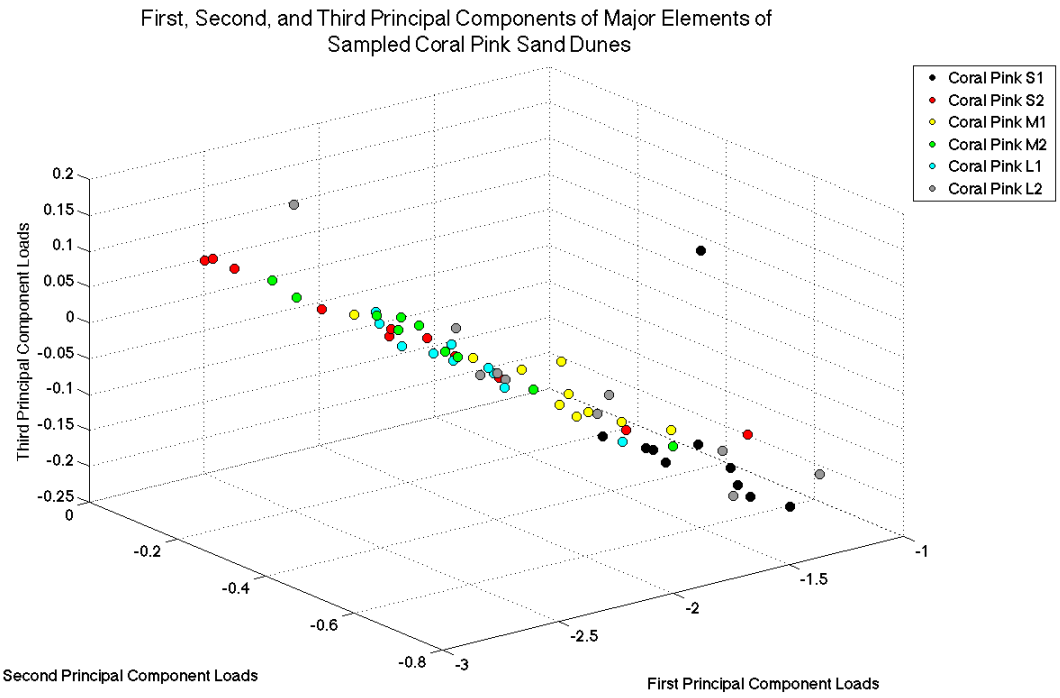

Figure 15. Plot of the first three principal components of major element data from the Coral Pink Sand Dunes. Note that all dunes overlap with other dunes, indicating a high degree of similarity. Note that the scale of the axes makes the data look more spread out than it really is. See Figure 12 to compare the spread of the different units to each other.

PCA of Trace Elements

When PCA is done on just trace elements (Ba, Ce, Cr, Cu, Ga, La, Nb, Nd, Ni, Pb, Rb, Sc, Sm, Sr, Th, U, V, Y, Zn, and Zr), the first three principal components describe 75.3% of the data – 51.1% from the first, 14.9% from the second, and 9.3% from the third. Every trace element except Ba contributed significantly to at least one of the first three principal components, with most of them contributing to the first principal component (Table 4).

Contributions of Major Elements to First Three Principle Components			
Element	**PCA 1 Contribution**	**PCA 2 Contribution**	**PCA 3 Contribution**
Ba	0.1348	0.0512	0.1323
Ce	0.2959	-0.0484	-0.0485
Cr	0.0062	0.5291	-0.1710
Cu	0.0334	0.5076	-0.1657
Ga	0.2838	-0.0060	0.1211
La	0.2866	-0.0130	-0.0369
Nb	0.2927	-0.0094	0.0242
Nd	0.1978	0.1564	0.4100
Ni	-0.0082	0.5405	-0.1754
Pb	0.2532	-0.0213	0.0375
Rb	0.2352	-0.0193	0.2019
Sc	0.1453	-0.1249	-0.5165
Sm	0.0975	0.1855	0.5580
Sr	0.2049	-0.0201	0.0617
Th	0.2845	-0.0494	-0.1031
U	0.2690	-0.0700	-0.2005
V	0.2825	0.0222	-0.0845
Y	0.2990	-0.0249	-0.0427
Zn	0.1383	0.2735	0.0151
Zr	0.2681	-0.0775	-0.1546

Table 4. Trace elements analyzed and relative contributions to the first three principal components. Elements with a significant contribution to a principal component are highlighted in green. Every trace element contributed significantly to at least one of the first three principal components except Ba.

Plots of the first three principal components of trace element data (Figures 16, 17, 18, and 19) were very similar in appearance to plots of all elements together. The branches of Weber Sandstone and Navajo Sandstone data were slightly more spread out, but the overall distribution and relationships between different units and dunes was similar (Compare Figures 7 and 16).

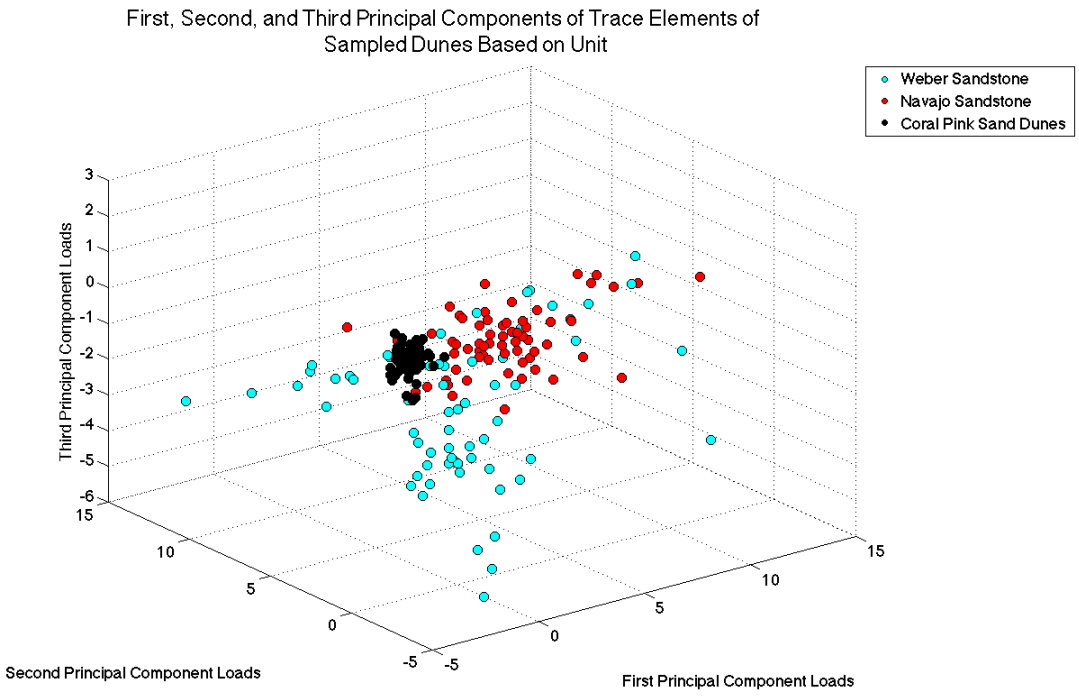

Figure 16. Plot of the first three principal components of trace element data from all units. The patterns in data distribution are similar to those in Figure 7 (all elements from all units), but the branches are more spread out and less distinct.

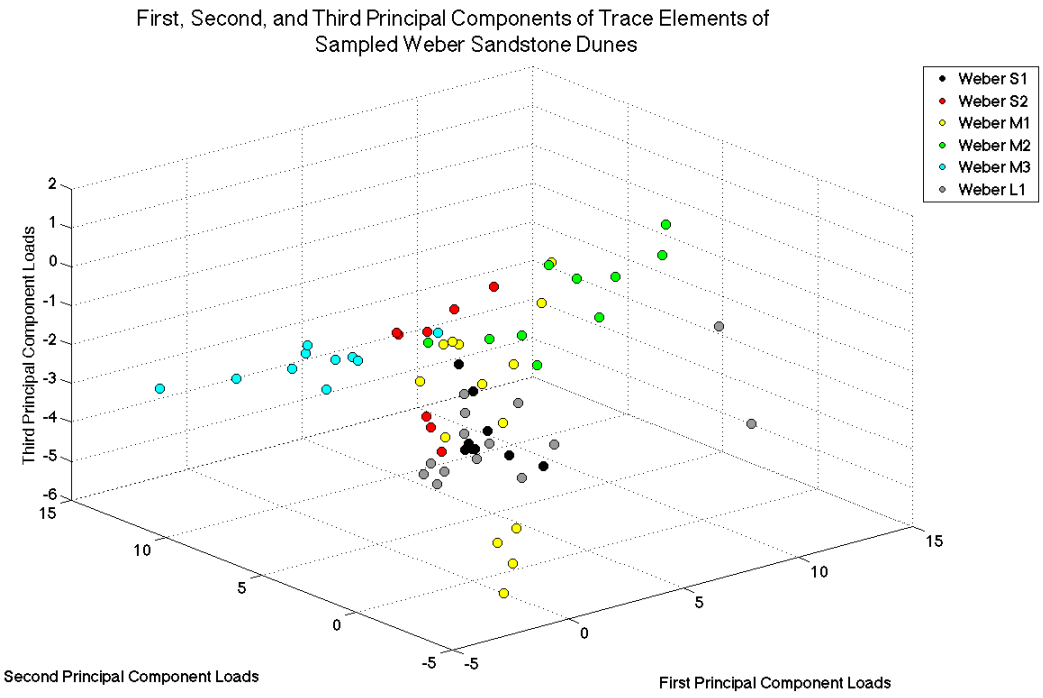

Figure 17. Plot of the first three principal components of trace element data from the Weber Sandstone, colored by dune. The distribution of data is similar to that of Figure 8 (all elements from the Weber Sandstone), with dunes having less overlap with each other than in the other units sampled. This indicates that the dunes can be highly dissimilar to each other compositionally.

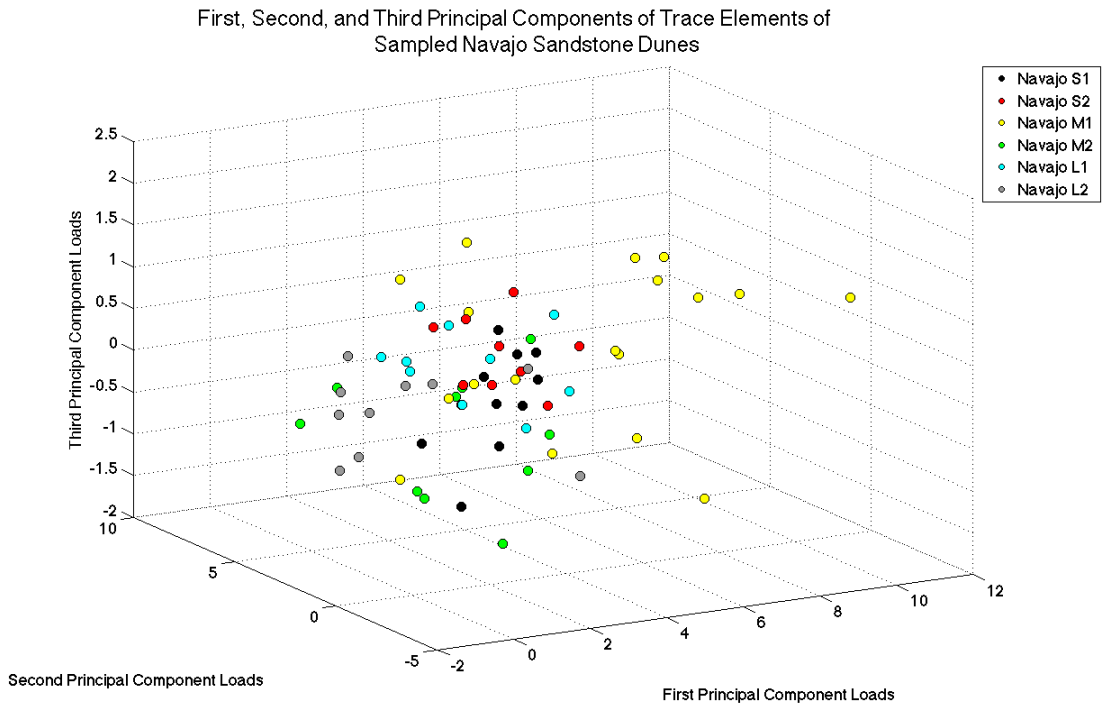

Figure 18. Plot of the first three principal components of trace element data from the Navajo Sandstone. Note that every dune sampled overlaps other sampled dunes, indicating a high degree of compositional similarity.

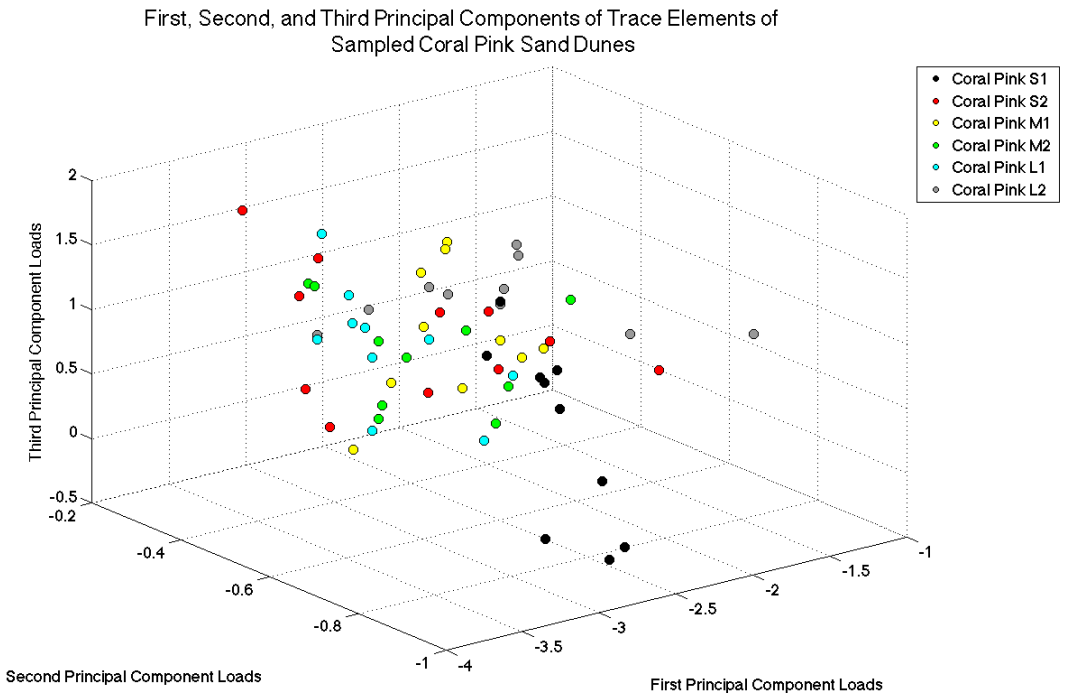

Figure 19. Plot of the first three principal components of trace element data from the Coral Pink Sand Dunes. Note that every dune sampled overlaps with other dunes, indicating a very high degree of compositional similarity. Note that the scale of the axes makes the data look more spread out than it really is. Figure 16 shows that sand of the Coral Pink Sand Dunes plots much more tightly than either the Weber or Navajo sandstones.

DISCUSSION

The original purpose of this study was to determine if trends in geochemistry exist along foreset laminae of eolian dunes in an effort to see if trends could be used to improve the quality of geochemical sampling and the estimation of paleodune preservation. Although this study indicates that there are not statistically significant trends to improve sampling quality or predict paleodune preservation, it does shed light on other facets of eolian geochemistry, potentially including effects of provenance and diagenesis on dune composition.

It had been expected that a combination of winnowing and kinetic sieve effects could lead to a concentration of some minerals with different hydraulic densities, such as concentrations of iron observed at the crests of other modern dunes (Boggs, 2012). The

sampling technique and analysis used in this study may not be able to reveal (or allow detection of) kinetic sieve effects within individual grainflow laminae that might have concentrated some minerals and their associated elements. However, it should have detected larger-scale separation of minerals along dune foresets, if they were present, that would likely be associated with this process. Such concentrations were not observed. The lack of such concentrations in the Coral Pink Sand Dunes may simply be due to the highly homogeneous nature of the grains in these dunes (nearly 98% SiO_2). There may not be enough non-quartz grains for such concentrations of other minerals to express themselves.

The Weber Sandstone is much more geochemically varied than either the Navajo Sandstone or the Coral Pink Sand Dunes. This may indicate that it is less compositionally mature than the other two units, possibly the result of a more complex depositional environment (with marine and fluvial influence in addition to an eolian environment) and a mixed provenance. Diagenetic effects such as cementation could also add to its complexity (Depret, 2005; Adams, 2006; Link et al., 2014). Distribution of Weber Sandstone data when plotted with principal components shows that differences between dunes can be as great or greater than differences within dunes. The geochemical data were grouped by dune, sometimes with little or no overlap, indicating that Weber Sandstone Dunes can be highly dissimilar compositionally. Because geochemical data from the Weber Sandstone shows that there can be significant differences in composition between individual dunes, a large number of samples from a large number of dunes may be needed to determine an accurate average composition for the eolian portions of this unit. No one dune, or any trends that may have been found in the dunes of this unit, would be able to represent the unit as a whole.

The Navajo Sandstone is less compositionally varied than the Weber Sandstone, with much more compositional overlap between the six dunes sampled. The Navajo Sandstone was deposited in a more uniform erg depositional environment (i.e. less fluvial and marine influence than the Weber Sandstone) with a less mixed provenance than the Weber Sandstone (Blakey, 1988; Dickinson and Gehrels, 2003; Rahl et al., 2003; Beitler et al., 2005; Campbell et al., 2005). Additionally, the grains in the Navajo Sandstone have been recycled more than once (Campbell et al., 2005), potentially making the Navajo Sandstone much "cleaner" than the Weber Sandstone. Not only is there less compositional variability in the Navajo Sandstone than the Weber Sandstone, but when the first three principal components of the Navajo Sandstone data were plotted, there was a large degree of compositional overlap between the dunes, even those from different areas. This means that any one sampled dune is likely to be like any other, and fewer samples would be needed to find an average composition of the unit than for units like the Weber Sandstone.

The active Coral Pink Sand Dunes of southern Utah are much less compositionally varied than either the Weber Sandstone or the Navajo Sandstone. Like the Navajo Sandstone, the Coral Pink Sand Dunes show a great deal of compositional overlap between the dunes within the unit. Sampling of just a few dunes may be sufficient to determine the average composition of the dunes.

The grains from the Coral Pink Sand Dunes are largely derived from the Navajo Sandstone, suggesting that even a partial turn of the rock cycle (weathering, erosion, and deposition) can significantly change eolian geochemistry, possibly through the elimination of less stable minerals and their associated elements (such as cements and feldspars). This may also suggest that diagenetic effects such as cementation play a significant role in compositional

variability (Phillips and Morris, 2012). The average SiO_2 concentration for the Navajo Sandstone is 92.0%, while the Coral Pink Sand Dunes average is 97.7% - a difference of nearly 6%. Major elements that dropped in concentration include Al_2O_3, Fe_2O_3, CaO, and K_2O. Weathering, erosion, and depositional processes may have caused physical and chemical breakdown or removal of cements and less stable mineral grains that contain these major elements, causing the increased concentration of SiO_2. Concentrations of all elements tested for and their averages can be found in Appendix A.

The Weber Sandstone and Navajo Sandstone have very similar concentrations of SiO_2, averaging 92.9% and 92.0% by weight, respectively. Despite this similarity in their most significant compositional constituent, principal components analysis (PCA) was able to illustrate differences between the two units, even when just major elements, including SiO_2, were used for calculations (see Figures 7 and 12). This shows that PCA may be viable as a method for use in other geochemical studies for distinguishing between different units that are similar to each other.

Because so many different elements contributed significantly to the first three principal components, it is difficult to determine any one cause for the distribution of the geochemical data in this study. Too many elements are involved in the principal components to find specific mineralogical or diagenetic causes for the differences between the Navajo and Weber sandstones or chemistry changes as the Navajo Sandstone erodes and is re-deposited as the Coral Pink Sand Dunes. Such determinations would require detailed petrographic work and sedimentologic study, possibly even lab studies of eolian processes, topics for a future study. Nonetheless, something intriguing about the distribution of the XRF elemental data sampled for this study when using PCA is that all of the converging branches of data are roughly centered around a

hypothetical point that likely represents 100% SiO_2. Because of this, PCA plots could potentially be used as an index of sandstone maturity.

CONCLUSIONS

This study found that there were no statistically significant, consistent patterns of geochemical change along the foresets of sampled dunes from the Weber Sandstone, Navajo Sandstone, or Coral Pink Sand Dunes. It also found that the length of a dune foreset did not control compositional variation.

Principal components analysis (PCA) was used to display and compare XRF elemental data from sampled dunes. This method revealed relationships in the data that would not be clear with a strictly numerical analysis. For example, PCA revealed three converging branches of the elemental data from the Weber Sandstone that may not otherwise have been observed (Figure 8).

When all elements were analyzed together, the first three principal components described 71.1% of the data. When PCA was done on just major or trace elements, the first three principal components described 80.1% and 75.5% of their respective data sets. Thus, PCA of major element data was able to describe more of the data than either the combined data or trace element data.

Plotting XRF data of all elements using principal components, the Weber Sandstone has the most compositional variety, and the Coral Pink Sand Dunes the least (Figure 7). Data from the Weber Sandstone was spread out between three converging branches. One of the three branches was comprised of data entirely from one dune, and another branch almost entirely from a different single dune. This shows that dunes within the Weber Sandstone can be significantly different compositionally, something that was not observed in the other two units. Geochemical

studies in the Weber Sandstone should sample a large number of dunes to achieve an accurate average of chemical composition.

Navajo Sandstone data from all elements, major elements, and trace elements plotted along or near one of the branches of Weber Sandstone data when using PCA (Figures 7, 12, and 16). When plotted, dunes in this unit all had significant overlap with other dunes in the same unit, indicating that they are all compositionally similar to each other. Geochemical studies of the Navajo Sandstone will require few samples to find an average chemical composition.

Data from the modern Coral Pink Sand Dunes (from all elements, major elements, and trace elements) plotted tightly in the area where the three branches converge (Figures 7, 12, and 16). Data from all dunes in this unit overlapped with all of the others using PCA, showing a very high level of compositional similarity. Few dunes would need to be sampled to determine an accurate average composition of the Coral Pink Sand Dunes.

When only XRF elemental data from trace elements was plotted using PCA, there were no significant changes to the relationships of the units and dunes sampled compared to when all elements were used. When only major element data was plotted, there was a significant change to the Weber Sandstone suite of data. One of the three branches, which had been comprised entirely of data from the Weber M3 dune, disappeared. The major element data from this dune plotted with the Coral Pink Sand Dunes data, in the area where the branches of Weber Sandstone data converge (compare Figures 8 and 13). This shows that, for at least one dune in the Weber Sandstone, the major and trace elements have distinct patterns, and both would probably need to be used in a study of geochemistry in the Weber Sandstone.

Future PCA and petrologic studies may focus on relating the major and trace elements to detrital or diagenetic makeup of the rock. For example, one may explore the trace elements that

create the third branch of the PCA trace element plot of the Weber Sandstone (see Figures 17 and 13). Are the contributing elements of this branch largely from detrital grains (i.e. provenance) or from diagenetic minerals? Studies of this nature may assist in determining the amount of provenance mixing by depositional processes verses basin-centered diagenetic influence.

Principal components analysis was found to be able to demonstrate a chemical difference between units. This includes differentiating between the Weber and Navajo sandstones, two quartz-dominated sandstones with similar SiO_2 content, with only major elements. Principal components analysis should therefore be a viable method for differentiating between similar units in other geochemistry studies.

REFERENCES

Adams, L.A., 2006, Sequence and mechanical stratigraphy; an integrated reservoir characterization of the weber sandstone, western Colorado (Ph.D. thesis): The University of Texas at El Paso, 116 p.

Beitler, B., Parry, W.T., and Chan, M.A., 2005, Fingerprints of fluid flow: chemical diagenetic history of the Jurassic Navajo sandstone, southern Utah, U.S.A.: Journal of Sedimentary Research, v. 75(4), p. 547-561.

Bissell, H. J., 1964, Lithology and petrography of the Weber Formation, in Utah and Colorado, Guidebook to the Geology and Mineral Resources of the Uinta Basin: Utah's Hydrocarbon Storehouse, Thirteenth Annual Field Conference, 1964, p. 67-91.

Blakey, R.C., Peterson, F., and Kocurek, G., 1988, Syntheses of late Paleozoic and Mesozoic eolian deposits of the western interior of the united states: Sedimentary Geology, v. 56(1-4), p. 3-125.

Boggs, S., Jr., 2012, Principles of Sedimentology and Stratigraphy: Upper Saddle River, Pearson Prentice Hall, 585 p.

Campbell, I.H., Reiners, P.W., Allen, C.M., Nicolescu, S., and Upadhyay, R., 2005, He-Pb double dating of detrital zircons from the Ganges and Indus rivers; implication for quantifying sediment recycling and provenance studies: Earth and Planetary Science Letters, v. 237(3-4), p. 402-432.

Chan, M.A., Parry, W.T., and Bowman, J.R., 2000, Diagenetic hematite and manganese oxides and fault-related fluid flow in Jurassic sandstones, southeastern Utah: AAPG Bulletin, v. 84(9), p. 1281-1310.

Crowell, J.C., 1978, Gondwanan glaciation, cyclothems, continental positioning, and climate change: American Journal of Science, v. 278(10), p. 1345-1372.

Dalrymple, A., and Morris, T.H., 2007, Facies analysis and reservoir characterization of outcrop analogs to the Navajo Sandstone in the central Utah thrust belt exploration play: Utah Geological Association Publication, v. 36, p. 311-322.

Depret, P., 2005, Reservoir characterization and tertiary recovery improvement of the Weber Sandstone, northwest Colorado (Ph.D. thesis): The University of Texas at El Paso, 129 p.

Dickinson, W.R., and Gehrels, G.E., 2003, U-Pb ages of detrital zircons from Permian and Jurassic eolian sandstones of the Colorado Plateau, USA: paleogeographic implications: Sedimentary Geology, v. 163(1-2), p. 29-66.

Eggett, D.L. Interview with Bickmore, B.R., Little, D.A., and Morris, T.H. Personal Interview. March 11, 2016.

Ford, R.L., and Gillman, S.L., 2000, Geology of Coral Pink Sand Dunes State Park, Kane County, Utah: Utah Geological Association Publication, v. 28, p. 365-389.

Fryberger, S.G., 1980 Eolian-fluviatile (continental) origin of ancient stratigraphic trap for petroleum in Weber Formation, Rangely Oil Field, Colorado: AAPG Bulletin, v. 64(5), p. 709-710.

Hintze, L.F., and Kowallis, B.J., 2009, Geologic History of Utah: Brigham Young University Geology Studies, Special Publication, 9, 225 p.

Hunter, R. E. (1977). Basic types of stratification in small eolian dunes: Sedimentology, v. 24(3), p. 361-387.

Kocurek, G., and Dott, R.H., Jr., 1981, Distinctions and uses of stratification types in the interpretation of eolian sand: Journal of Sedimentary Petrology, v. 51(2), p. 579-595.

Link, P.K., Mahon, R.C., Beranek, L.P., Campbell-Stone, E., and Lynds, R., 2014, Detrital zircon provenance of Pennsylvanian to Permian sandstones from the Wyoming craton and Wood River Basin, Idaho, U.S.A.: Rocky Mountain Geology, v. 49(2), p. 115-136.

McKillup, S., and Dyar, M.D., 2010, Geostatistics Explained: An Introductory Guide for Earth Scientists: Cambridge, Cambridge University Press, 396 p.

Phillips, S.P., 2012, Discriminant analysis of XRF data from sandstones of like facies and appearance: A method for identifying a regional unconformity, paleotopography,and diagenetic histories [MS thesis] : Brigham Young University, 121 p.

Rahl, J.M., Reiners, P.W., Campbell, I.H., Nicolescu, S., and Allen, C.M., 2003, Combined single-grain (U-Th)/He and U/Pb dating of detrital zircons from the Navajo Sandstone, Utah: Geology (Boulder), v. 31(9), p. 761-764.

Trauth, M.H., 2010, MATLAB Recipes for Earth Scientists: Berlin, Springer-Verlag, 336 p.

Utah Oral Health Program: My Water's Fluoride: http://health.utah.gov/oralhealth/fluoride.php (accessed October 2016).

APPENDICES

Appendix A: XRF Data

The tables in this appendix contain the names, positions (see Figure 2), and major and trace element concentrations for samples taken.

Weber Sandstone Major Element XRF Data												
Sample Name	Sample Position	Foreset Length (inches)	Major Elements - Concentration in Weight Percent									
			SiO2	TiO2	Al2O3	Fe2O3	MnO	MgO	CaO	Na2O	K2O	P2O5
PPwS1S1	1	0.0	92.42	0.07	1.80	0.28	0.00	0.57	1.77	0.00	0.68	0.02
PPwS1S2	2	21.0	91.80	0.06	1.60	0.22	0.00	0.76	2.08	0.00	0.61	0.01
PPwS1S3	3	42.0	88.16	0.06	1.52	0.24	0.00	0.89	4.04	0.00	0.57	0.02
PPwS1S4	4	63.0	95.36	0.05	1.54	0.25	0.01	0.17	0.75	0.00	0.57	0.02
PPwS1S5	5	84.0	89.73	0.07	1.63	0.31	0.00	1.14	2.72	0.00	0.61	0.02
PPwS1S6	6	105.0	90.88	0.05	1.36	0.21	0.00	0.78	2.81	0.00	0.53	0.01
PPwS1S7G	7	126.0	85.64	0.11	1.95	0.31	0.01	1.90	3.81	0.00	0.75	0.02
PPwS1S8G	8	147.0	90.05	0.07	1.46	0.31	0.00	0.94	2.93	0.00	0.55	0.02
PPwS1S9G	9	168.0	89.96	0.06	1.50	0.24	0.00	1.00	2.95	0.00	0.57	0.01
PPwS1S10G	10	189.0	90.10	0.06	1.39	0.22	0.00	0.98	2.99	0.00	0.53	0.01
PPwS2S1	1	0.0	96.45	0.05	1.44	0.28	0.00	0.02	0.10	0.00	0.51	0.02
PPwS2S2	2	21.0	96.14	0.09	1.83	0.36	0.00	0.03	0.18	0.00	0.65	0.01
PPwS2S3	3	42.0	98.25	0.02	0.57	0.13	0.00	0.00	0.35	0.00	0.15	0.01
PPwS2S4	4	63.0	98.74	0.02	0.45	0.09	0.00	0.00	0.23	0.00	0.12	0.01
PPwS2S5	5	84.0	93.82	0.01	0.74	0.16	0.00	0.03	2.17	0.00	0.24	0.01
PPwS2S6	6	105.0	92.66	0.02	0.78	0.21	0.00	0.04	3.21	0.00	0.26	0.01
PPwS2S7	7	126.0	90.02	0.02	0.94	0.26	0.01	0.08	4.78	0.00	0.32	0.01
PPwS2S8A	8	147.0	93.75	0.02	0.68	0.18	0.00	0.04	2.72	0.00	0.22	0.01
PPwS2S9	9	168.0	97.23	0.03	0.78	0.60	0.00	0.02	0.28	0.00	0.25	0.01
PPwS2S10	10	189.0	96.13	0.02	1.01	0.25	0.00	0.03	0.98	0.00	0.36	0.01
PPwM1S1	1	0.0	92.02	0.10	2.34	1.07	0.00	0.09	0.29	2.10	1.03	0.02
PPwM1S1A	1	0.0	91.09	0.13	2.34	2.17	0.00	0.07	0.10	2.26	0.94	0.03
PPwM1S3	3	64.0	93.89	0.12	1.78	0.34	0.00	0.35	1.17	0.00	0.66	0.02
PPwM1S4	4	96.0	81.39	0.07	1.41	0.40	0.01	0.13	8.81	0.00	0.52	0.02
PPwM1S4A	4	96.0	81.11	0.08	1.60	0.38	0.01	0.13	8.80	0.00	0.61	0.02
PPwM1S4B	4	96.0	84.26	0.06	1.22	0.36	0.01	0.11	7.31	0.00	0.45	0.02
PPwM1S4C	4	96.0	85.06	0.08	1.33	0.40	0.01	0.23	6.68	0.00	0.48	0.02
PPwM1S6	6	160.0	92.36	0.08	1.61	0.38	0.00	0.06	2.48	0.00	0.60	0.02
PPwM1S7	7	192.0	95.17	0.03	0.97	0.17	0.00	0.02	1.59	0.00	0.32	0.02
PPwM1S7A	7	192.0	94.03	0.04	1.11	0.18	0.00	0.04	2.20	0.00	0.39	0.02
PPwM1S8	8	224.0	93.80	0.08	1.61	0.28	0.00	0.05	1.71	0.00	0.60	0.03
PPwM1S8A	8	224.0	94.81	0.05	1.27	0.23	0.00	0.03	1.58	0.00	0.46	0.02
PPwM1S9	9	256.0	96.92	0.04	1.04	0.19	0.00	0.01	0.63	0.00	0.36	0.02
PPwM1S10	10	288.0	96.03	0.06	1.58	0.26	0.00	0.04	0.55	0.00	0.63	0.02
PPwM2S1A	1	0.0	93.48	0.22	3.47	0.20	0.00	0.09	0.25	0.00	1.20	0.02
PPwM2S2B	2	54.5	91.39	0.30	4.15	0.79	0.00	0.09	0.22	0.00	1.42	0.02
PPwM2S3	3	109.0	91.33	0.24	4.68	0.84	0.00	0.09	0.04	0.00	1.51	0.02
PPwM2S4	4	163.5	92.06	0.21	4.47	0.47	0.00	0.08	0.05	0.00	1.53	0.02
PPwM2S5	5	218.0	95.59	0.05	1.75	0.11	0.00	0.08	0.68	0.00	0.62	0.01
PPwM2S6	6	272.5	96.54	0.09	1.95	0.09	0.00	0.03	0.00	0.00	0.70	0.01
PPwM2S7	7	327.0	93.97	0.12	3.03	0.28	0.00	0.06	0.32	0.00	1.11	0.02
PPwM2S8A	8	381.5	93.91	0.18	3.20	0.45	0.00	0.07	0.07	0.00	1.05	0.02
PPwM2S9A	9	436.0	94.60	0.18	3.00	0.15	0.00	0.06	0.09	0.00	0.99	0.02
PPwM2S10A	10	490.5	94.42	0.11	2.62	0.51	0.00	0.06	0.33	0.00	0.87	0.03
PPwM3S1	1	0.0	98.12	0.02	0.80	0.08	0.00	0.00	0.00	0.00	0.20	0.01
PPwM3S2	2	44.2	98.48	0.00	0.25	0.23	0.00	0.03	0.02	0.00	0.11	0.01
PPwM3S3	3	88.4	98.06	0.01	0.28	0.22	0.00	0.12	0.06	0.00	0.12	0.01
PPwM3S4	4	132.6	98.24	0.00	0.22	0.05	0.00	0.03	0.18	0.00	0.03	0.01
PPwM3S5	5	176.8	98.33	0.00	0.24	0.13	0.00	0.05	0.06	0.00	0.05	0.01
PPwM3S6	6	221.0	99.01	0.00	0.18	0.12	0.00	0.00	0.08	0.00	0.02	0.01
PPwM3S7	7	265.2	99.08	0.01	0.22	0.11	0.00	0.00	0.03	0.00	0.03	0.01
PPwM3S8	8	309.4	98.64	0.01	0.25	0.20	0.00	0.00	0.00	0.00	0.04	0.01
PPwM3S9	9	353.6	97.78	0.01	0.36	0.40	0.02	0.00	0.06	0.00	0.06	0.02
PPwM3S10	10	379.8	97.91	0.01	0.33	0.41	0.01	0.00	0.00	0.00	0.06	0.01
PPwL1S1	1	0.0	85.42	0.24	3.55	0.75	0.01	0.18	4.12	0.00	1.35	0.04
PPwL1S2	2	116.0	90.07	0.10	2.00	0.48	0.01	0.08	3.36	0.00	0.76	0.02
PPwL1S3	3	232.0	91.72	0.07	1.44	0.37	0.00	0.05	2.90	0.00	0.52	0.02
PPwL1S4	4	348.0	91.50	0.25	2.95	0.65	0.00	0.08	1.35	0.00	1.01	0.04
PPwL1S5	5	464.0	91.79	0.05	1.70	0.48	0.00	0.05	2.42	0.00	0.68	0.02
PPwL1S5A	5	464.0	92.27	0.04	1.70	0.48	0.00	0.04	2.35	0.00	0.67	0.01
PPwL1S6	6	580.0	90.72	0.06	1.59	0.26	0.01	0.06	3.41	0.00	0.63	0.01
PPwL1S7	7	696.0	90.03	0.09	2.30	0.41	0.01	0.07	3.09	0.00	0.93	0.02
PPwL1S8	8	812.0	91.25	0.02	1.03	0.14	0.01	0.04	3.82	0.00	0.40	0.01
PPwL1S8A	8	812.0	89.21	0.09	2.03	0.34	0.01	0.08	3.87	0.13	0.76	0.02
PPwL1S8B	8	812.0	91.01	0.03	1.27	0.26	0.01	0.05	3.67	0.00	0.50	0.01
PPwL1S9	9	928.0	90.96	0.02	1.04	0.20	0.01	0.04	3.79	0.00	0.40	0.01
PPwL1S9A	9	928.0	90.02	0.03	1.07	0.26	0.01	0.05	4.45	0.00	0.41	0.01
PPwL1S10A	10	1044.0	90.51	0.07	1.92	0.08	0.00	0.06	3.43	0.00	0.80	0.01
		Average Concentration	92.89	0.07	1.58	0.34	0.00	0.19	1.98	0.07	0.57	0.02

Weber Sandstone Trace Element XRF Data																							
Sample Name	Sample Position	Foreset Length (inches)	Trace Elements - Concentration in Parts Per Million																				
			Ba	Ce	Cr	Cu	Ga	La	Nb	Nd	Ni	Pb	Rb	Sc	Sm	Sr	Th	U	V	Y	Zn	Zr
PPwS1S1	1	0.0	89	8	8	25	3	5	1	8	5	3	16	1	3	26	1	1	6	3	4	126
PPwS1S2	2	21.0	84	6	6	12	3	4	1	5	5	3	14	2	2	24	1	1	6	3	3	98
PPwS1S3	3	42.0	92	3	7	1	3	4	1	3	5	3	14	2	2	31	1	1	6	3	3	106
PPwS1S4	4	63.0	90	8	8	2	3	3	1	8	6	3	13	1	3	19	1	1	6	3	4	88
PPwS1S5	5	84.0	86	9	9	2	3	5	1	4	6	4	15	2	2	29	2	2	6	4	4	155
PPwS1S6	6	105.0	77	4	5	2	3	3	1	5	4	3	13	2	2	21	1	1	6	3	3	78
PPwS1S7G	7	126.0	90	9	9	0	3	8	2	5	4	4	18	3	2	33	2	2	8	5	4	206
PPwS1S8G	8	147.0	76	5	7	0	3	6	1	6	6	3	13	2	2	25	1	1	7	3	3	132
PPwS1S9G	9	168.0	82	5	6	14	3	4	1	4	6	3	14	2	2	27	1	1	5	3	4	131
PPwS1S10G	10	189.0	75	6	6	1	3	4	1	4	5	2	13	2	2	24	1	1	5	3	3	90
PPwS2S1	1	0.0	75	7	9	4	3	4	1	10	7	2	12	0	3	20	1	1	8	3	9	96
PPwS2S2	2	21.0	83	10	13	1	3	5	1	12	6	4	15	0	4	26	2	2	10	3	19	130
PPwS2S3	3	42.0	32	0	5	1	2	3	0	7	7	1	5	0	3	11	0	0	3	1	5	29
PPwS2S4	4	63.0	30	3	4	4	2	2	0	8	5	1	4	0	3	10	0	0	3	1	4	23
PPwS2S5	5	84.0	48	2	5	4	2	4	1	4	6	1	7	2	3	16	0	0	5	2	5	35
PPwS2S6	6	105.0	50	2	5	8	3	4	1	4	6	1	7	2	2	19	0	1	6	2	6	47
PPwS2S7	7	126.0	53	4	6	1	3	4	1	8	7	1	9	2	3	21	1	1	3	2	14	58
PPwS2S8A	8	147.0	47	1	4	14	2	3	1	5	6	2	6	2	2	20	1	1	5	2	5	36
PPwS2S9	9	168.0	44	4	10	10	2	4	1	9	12	3	7	0	3	15	1	1	6	2	12	48
PPwS2S10	10	189.0	44	3	5	0	3	5	1	4	6	1	8	5	2	26	1	1	2	3	6	58
PPwM1S1	1	0.0	124	15	13	2	3	7	2	11	14	8	20	1	4	31	2	2	12	4	17	204
PPwM1S1A	1	0.0	106	14	31	5	3	8	2	15	11	8	19	0	4	32	3	2	13	5	17	252
PPwM1S3	3	64.0	85	13	17	6	3	6	1	10	8	4	15	1	3	28	2	2	7	4	5	195
PPwM1S4	4	96.0	71	7	9	2	3	4	1	0	4	4	13	1	0	29	1	2	8	4	4	128
PPwM1S4A	4	96.0	82	6	12	12	3	5	2	0	7	4	15	2	0	30	1	2	11	4	6	153
PPwM1S4B	4	96.0	66	11	5	0	3	6	1	0	3	3	12	2	1	24	2	2	8	4	2	116
PPwM1S4C	4	96.0	138	6	18	2	2	4	1	1	14	4	12	5	1	24	1	2	9	4	3	126
PPwM1S6	6	160.0	74	9	13	1	3	5	1	7	7	4	14	1	2	24	2	2	8	3	2	143
PPwM1S7	7	192.0	46	2	3	2	2	2	1	5	5	2	8	1	3	18	0	0	5	1	2	54
PPwM1S7A	7	192.0	57	4	15	2	2	4	1	4	8	2	10	1	2	20	1	1	5	2	3	60
PPwM1S8	8	224.0	88	7	9	19	3	4	1	7	7	3	14	1	3	24	2	2	6	3	3	136
PPwM1S8A	8	224.0	64	7	7	0	3	5	1	8	6	2	11	0	3	19	0	1	5	2	2	87
PPwM1S9	9	256.0	53	4	6	3	3	3	1	8	6	2	9	0	3	17	1	1	4	2	2	57
PPwM1S10	10	288.0	88	5	5	0	3	4	1	7	7	3	15	0	3	26	1	1	6	2	2	71
PPwM2S1A	1	0.0	110	22	32	73	5	10	3	12	7	7	28	1	4	44	4	3	18	7	5	283
PPwM2S2B	2	54.5	2413	19	41	16	5	12	4	17	5	4	33	1	4	63	4	3	23	7	5	292
PPwM2S3	3	109.0	121	23	43	6	6	11	4	16	8	6	34	1	4	62	5	3	21	7	6	315
PPwM2S4	4	163.5	134	20	33	9	6	12	3	13	6	6	34	1	4	63	2	2	21	6	4	163
PPwM2S5	5	218.0	179	4	17	82	3	7	1	8	5	3	14	1	3	27	1	1	9	2	2	72
PPwM2S6	6	272.5	80	9	19	3	3	6	1	9	5	3	16	0	3	25	2	2	9	3	3	126
PPwM2S7	7	327.0	119	12	19	8	4	8	2	9	5	3	24	2	3	36	2	2	13	4	4	119
PPwM2S8A	8	381.5	1317	13	22	10	4	8	2	12	6	4	24	1	4	44	1	1	18	5	3	141
PPwM2S9A	9	436.0	91	17	27	1	5	11	3	13	5	3	23	0	4	51	3	2	16	6	3	197
PPwM2S10A	10	490.5	294	13	20	14	4	7	2	10	7	5	20	1	3	34	1	1	15	5	4	105
PPwM3S1	1	0.0	24	1	7	0	2	4	1	8	6	5	5	0	3	10	0	1	8	2	9	49
PPwM3S2	2	44.2	24	0	157	55	2	0	0	8	48	1	2	0	3	6	0	0	3	1	6	19
PPwM3S3	3	88.4	20	0	152	42	3	3	1	8	47	0	3	0	3	9	0	0	3	1	13	22
PPwM3S4	4	132.6	25	1	30	34	1	2	0	9	19	1	2	0	3	8	0	1	2	1	5	17
PPwM3S5	5	176.8	20	0	105	26	2	2	1	7	35	1	3	0	3	7	0	0	2	1	5	21
PPwM3S6	6	221.0	34	0	130	20	1	3	0	6	31	0	2	0	3	5	0	0	3	1	2	18
PPwM3S7	7	265.2	18	0	75	30	2	2	0	9	30	6	2	0	3	6	0	0	1	1	5	20
PPwM3S8	8	309.4	18	0	144	59	2	4	1	9	50	2	2	0	3	7	0	0	2	1	4	22
PPwM3S9	9	353.6	61	0	320	72	2	4	1	8	84	2	3	0	3	7	0	1	5	1	10	22
PPwM3S10	10	379.8	24	0	372	121	2	2	1	9	108	1	3	0	3	6	0	0	4	1	9	20
PPwL1S1	1	0.0	163	34	23	13	5	13	3	14	11	9	32	4	3	59	7	4	18	11	5	516
PPwL1S2	2	116.0	100	11	13	1	4	4	2	7	8	3	18	1	2	31	2	2	10	4	4	168
PPwL1S3	3	232.0	74	6	7	28	3	5	1	4	7	3	13	1	2	24	1	1	10	3	4	89
PPwL1S4	4	348.0	105	33	23	1	5	13	3	16	9	8	23	1	4	55	7	5	17	8	4	540
PPwL1S5	5	464.0	95	3	7	0	3	2	1	5	9	5	16	2	2	23	1	1	8	2	7	70
PPwL1S5A	5	464.0	89	2	7	2	3	3	1	4	9	5	15	1	3	23	1	1	6	2	6	76
PPwL1S6	6	580.0	87	2	5	1	3	5	1	3	5	4	15	3	2	23	1	1	8	3	5	65
PPwL1S7	7	696.0	124	13	9	4	3	7	1	6	7	6	21	3	2	31	3	2	11	3	8	224
PPwL1S8	8	812.0	61	1	4	0	2	4	1	2	5	2	10	2	2	17	1	1	5	2	5	24
PPwL1S8A	8	812.0	99	11	10	10	4	6	1	3	7	3	18	2	2	31	2	2	11	4	4	189
PPwL1S8B	8	812.0	76	3	16	0	3	2	1	0	8	3	12	1	2	19	0	0	7	2	7	36
PPwL1S9	9	928.0	60	0	10	10	2	3	1	1	6	3	10	1	2	16	0	0	6	2	5	29
PPwL1S9A	9	928.0	65	0	4	0	3	3	1	0	5	3	10	2	2	17	0	0	5	2	5	32
PPwL1S10A	10	1044.0	112	8	9	0	3	4	1	3	4	2	19	2	2	27	1	1	9	2	3	112
		Average Concentration	131.20	7.20	32.46	13.39	2.96	4.97	1.19	6.94	12.41	3.27	13.46	1.20	2.67	25.03	1.32	1.23	7.95	3.03	5.40	114.17

Navajo Sandstone Major Element XRF Data												
Sample Name	Sample Position	Foreset Length (inches)	Major Elements - Concentration in Weight Percent									
			SiO2	TiO2	Al2O3	Fe2O3	MnO	MgO	CaO	Na2O	K2O	P2O5
JnS1S1	1	0	89.274	0.092	2.504	0.935	0.028	1.086	1.566	0	1.068	0.025
JnS1S2	2	21.3	86.452	0.063	3.004	0.561	0.019	0.535	0.761	0	1.247	0.024
JnS1S3	3	42.6	88.691	0.109	3.889	0.592	0.02	0.842	1.152	0.047	1.67	0.036
JnS1S4	4	63.9	90.469	0.099	3.959	0.401	0.012	0.496	0.669	0.004	1.716	0.036
JnS1S5	5	85.2	91.149	0.106	4.27	0.328	0.009	0.264	0.32	0.001	1.818	0.04
JnS1S6	6	106.5	91.102	0.079	4.067	0.303	0.014	0.283	0.587	0.014	1.767	0.035
JnS1S7	7	127.8	91.594	0.105	4.092	0.268	0.003	0.212	0.232	0	1.782	0.037
JnS1S8	8	149.1	91.984	0.094	4.286	0.332	0.002	0.118	0.053	0.006	1.819	0.042
JnS1S9	9	170.4	91.737	0.111	4.21	0.223	0.001	0.175	0.084	0.028	1.821	0.038
JnS1S10	10	191.7	92.269	0.09	4.108	0.2	0	0.132	0.059	0.01	1.824	0.032
JnS2S1	1	0	93.274	0.111	3.221	0.376	0.006	0.177	0.031	0.009	1.315	0.036
JnS2S2	2	24.2	92.284	0.132	3.438	0.378	0.001	0.184	0.291	0.04	1.459	0.041
JnS2S3	3	48.4	93.409	0.072	3.167	0.326	0	0.141	0.014	0.024	1.462	0.031
JnS2S4	4	72.6	92.86	0.061	3.399	0.424	0.001	0.132	0.075	0.025	1.58	0.034
JnS2S5	5	96.8	91.991	0.072	3.796	0.362	0.001	0.123	0.138	0.025	1.784	0.037
JnS2S6	6	121	91.667	0.09	4.017	0.275	0.001	0.211	0.068	0.048	1.853	0.039
JnS2S7	7	145.2	91.485	0.106	4.127	0.317	0.001	0.208	0.047	0.036	1.869	0.04
JnS2S8	8	169.4	91.425	0.08	4.056	0.489	0.001	0.224	0.081	0.022	1.832	0.039
JnS2S9	9	193.6	91.201	0.119	4.158	0.259	0.001	0.172	0.241	0.016	1.85	0.039
JnS2S10	10	217.8	90.821	0.125	4.559	0.279	0.002	0.241	0.068	0.021	1.956	0.045
JnM1S1	1	0	90.47	0.21	4.88	0.51	0.01	0.17	0.13	0.04	2.48	0.07
JnM1S1A	1	0	88.12	0.36	4.84	0.91	0.02	0.41	0.86	0.03	2.49	0.08
JnM1S1B	1	0	89.80	0.22	4.42	0.64	0.02	0.30	0.64	0.03	2.21	0.05
JnM1S2	2	76	91.04	0.25	4.32	0.71	0.01	0.18	0.25	0.02	1.99	0.05
JnM1S3	3	152	90.78	0.20	3.80	0.87	0.01	0.19	0.41	0.03	1.69	0.05
JnM1S3A	3	152	89.40	0.26	4.63	0.95	0.01	0.22	0.52	0.03	2.21	0.05
JnM1S3B	3	152	90.42	0.25	4.19	0.91	0.01	0.22	0.28	0.03	1.89	0.06
JnM1S4	4	228	92.84	0.09	2.39	0.83	0.02	0.18	0.76	0.00	1.13	0.03
JnM1S4B	4	228	87.16	0.29	3.99	0.80	0.01	0.74	2.02	0.02	1.96	0.05
JnM1S5	5	304	89.56	0.05	2.27	0.79	0.03	0.25	2.97	0.00	1.03	0.02
JnM1S5A	5	304	87.84	0.28	4.46	1.69	0.02	0.48	0.72	0.02	2.28	0.06
JnM1S6	6	380	93.83	0.05	2.07	0.42	0.01	0.22	0.95	0.00	0.95	0.02
JnM1S6B	6	380	88.81	0.22	3.47	0.64	0.02	0.64	1.66	0.02	1.77	0.05
JnM1S7	7	456	91.86	0.15	2.67	0.42	0.02	0.54	1.07	0.00	1.31	0.03
JnM1S8	8	532	92.42	0.09	2.63	0.40	0.01	0.30	0.83	0.00	1.18	0.03
JnM1S8A	8	532	92.68	0.09	2.64	0.43	0.02	0.32	0.75	0.00	1.19	0.03
JnM1S9	9	608	92.45	0.12	2.77	0.47	0.01	0.35	0.78	0.00	1.27	0.03
JnM1S10	10	684	92.92	0.16	3.12	0.35	0.01	0.29	0.43	0.00	1.49	0.04
JnM2S1	1.00	0.00	96.11	0.05	1.81	0.19	0.00	0.05	0.16	0.00	1.05	0.02
JnM2S3	3.00	82.50	91.90	0.13	2.88	0.52	0.03	0.28	1.09	0.00	1.47	0.04
JnM2S3	3.00	165.00	94.39	0.07	2.17	0.41	0.02	0.09	0.30	0.00	1.11	0.03
JnM2S4	4.00	247.50	90.40	0.09	2.70	0.45	0.02	0.34	2.09	0.00	1.38	0.03
JnM2S5	5.00	330.00	92.11	0.09	2.90	1.13	0.02	0.25	0.58	0.00	1.47	0.04
JnM2S6	6.00	412.50	93.51	0.07	3.04	0.32	0.01	0.15	0.39	0.00	1.59	0.04
JnM2S7	7.00	495.00	92.38	0.08	2.94	0.33	0.01	0.20	1.00	0.00	1.54	0.03
JnM2S8	8.00	577.50	93.01	0.11	3.52	0.34	0.01	0.12	0.05	0.00	1.88	0.04
JnM2S9	9.00	660.00	93.83	0.08	3.12	0.24	0.01	0.12	0.11	0.00	1.64	0.03
JnM2S10	10.00	742.50	93.09	0.09	3.18	0.46	0.01	0.20	0.30	0.00	1.57	0.04
JnL1S1	1	0	93.54	0.043	3.128	0.349	0.001	0.048	0.178	0	2.071	0.022
JnL1S2	2	216	92.375	0.082	3.028	0.548	0.011	0.129	0.493	0	1.943	0.024
JnL1S3	3	432	92.769	0.078	3.282	0.506	0.008	0.048	0.149	0	2.09	0.023
JnL1S4	4	648	93.627	0.021	2.897	0.195	0.002	0.041	0.18	0.023	1.913	0.018
JnL1S5	5	864	94.637	0.023	2.312	0.145	0.002	0.042	0.279	0	1.548	0.017
JnL1S6	6	1080	93.939	0.036	2.757	0.208	0.001	0.023	0.129	0	1.817	0.016
JnL1S7	7	1296	94.481	0.014	2.596	0.162	0.002	0.013	0.174	0	1.772	0.017
JnL1S8	8	1512	94.284	0.04	3.046	0.214	0.002	0.03	0	0	1.979	0.018
JnL1S9	9	1728	92.186	0.133	3.567	0.332	0.004	0.121	0.236	0.001	2.291	0.022
JnL1S10	10	1944	93.271	0.057	3.186	0.257	0.004	0.084	0.202	0	2.07	0.019
JnL2S1	1	0	93.274	0.055	2.046	0.257	0.014	0.56	0.882	0	0.792	0.021
JnL2S2	2	159.6	93.701	0.039	1.594	0.264	0.012	0.508	1.001	0	0.638	0.017
JnL2S3	3	319.2	94.294	0.029	1.074	0.332	0.015	0.563	1.171	0	0.291	0.013
JnL2S4	4	478.8	93.781	0.023	1.329	0.316	0.013	0.512	1.178	0	0.473	0.016
JnL2S5	5	638.4	95.131	0.001	1.576	0.204	0.008	0.267	0.638	0	0.587	0.015
JnL2S6	6	798	94.936	0.03	2.266	0.174	0.005	0.133	0.254	0	0.995	0.019
JnL2S7	7	957.6	95.485	0.031	2.282	0.158	0.003	0.056	0.029	0.306	1.014	0.018
JnL2S8	8	1117.2	93.935	0.061	2.379	0.19	0.006	0.202	0.352	0	0.954	0.023
JnL2S9	9	1276.8	89.178	0.136	3.523	0.407	0.018	0.744	1.354	0	1.581	0.031
JnL2S10	10	1436.4	91.277	0.115	3.802	0.272	0.009	0.324	0.518	0	1.555	0.025
		Average Concentration	92.03	0.11	3.23	0.44	0.01	0.27	0.56	0.01	1.57	0.03

Navajo Sandstone Trace Element XRF Data																							
Sample Name	Sample Position	Foreset Length (inches)	Trace Elements - Concentration in Parts Per Million																				
			Ba	Ce	Cr	Cu	Ga	La	Nb	Nd	Ni	Pb	Rb	Sc	Sm	Sr	Th	U	V	Y	Zn	Zr
JnS1S1	1	0	1224.3	7.5	77.2	40.2	3.1	4.7	1.5	8.6	34.4	5.1	28.3	2.8	2.9	54.6	1.9	1.3	12.1	5.1	36.4	116
JnS1S2	2	21.3	814.3	4.9	25.7	22.8	3.3	3.4	1.3	7.4	15.9	3.6	32.7	1.6	2.6	51.5	0.3	0.6	9.8	4.3	23.8	72
JnS1S3	3	42.6	905.2	5.6	10.8	8.7	4.1	5.2	1.6	7.6	6.9	5.8	42.2	2.1	3	72.1	1.3	1.3	10.2	5.3	24	98.6
JnS1S4	4	63.9	303.3	7	14.1	8.3	4.1	5.3	1.6	7.7	6.5	6.1	43.6	1.4	2.9	67.4	1.2	1	9.4	4.5	16.5	90.6
JnS1S5	5	85.2	319.4	10.2	15.9	11.4	4.3	7.4	2	10.1	7.2	6.3	46.3	0.6	2.8	76.4	1.7	1.3	8.5	5.4	13.9	122.2
JnS1S6	6	106.5	338.9	9	11.1	7.5	4.2	5.4	1.6	7.2	5.7	5.6	45.2	1.7	2.5	72.7	0.8	0.8	8.5	4.8	11.7	86.3
JnS1S7	7	127.8	317.4	8.2	37.9	31.8	4.3	6.4	1.6	8.6	16.1	6	46.5	0.8	3	77.4	1.2	1.2	8.5	4.7	16.4	102.9
JnS1S8	8	149.1	316.5	11.5	15	12.1	4.5	8.8	1.9	8.2	6.9	6.3	46.7	0.6	2.7	82.5	1.6	1.3	7.2	5	11.6	115.9
JnS1S9	9	170.4	319.1	10.6	11.3	5.2	4.3	6.1	1.7	7.9	5.6	5.8	47.3	0.9	3.1	86	1.3	1.1	7.5	4.5	7.9	101.2
JnS1S10	10	191.7	314.1	8.2	13.2	6	4.5	4.9	1.7	9	5.7	6	46.6	0.4	2.9	80.9	1	1.1	8.7	3.9	7.8	91.2
JnS2S1	1	0	224.1	11.4	12.7	9.1	3.6	6.6	1.7	9.6	8.8	4.5	31.9	0.4	2.8	64.2	1.4	1.2	10.2	4.7	9.9	109.1
JnS2S2	2	24.2	242.2	13.2	15.3	6.4	4.3	6.2	2	8.3	6.2	5.4	36.1	1.5	3.3	77.8	2.2	1.5	11	5.2	10.2	134.5
JnS2S3	3	48.4	259.6	6.8	11	6.3	3.8	6.3	1.2	9	6.4	4.9	36.3	0.2	3.3	61.1	1	1.1	8.9	4	7.7	80.5
JnS2S4	4	72.6	274.3	8.5	46.1	20.6	3.9	6	1.3	8.2	17.9	5.2	39.3	0.4	2.8	68.9	1.5	1.5	9.3	4.2	8.3	63.5
JnS2S5	5	96.8	301.8	6.5	50.2	28.4	4.3	4.9	1.5	8.1	21.2	5.5	44.1	0.2	3.2	76.4	0.7	0.6	8.5	4.3	11.9	56.5
JnS2S6	6	121	310.1	8	27.6	14.6	4.1	5.7	1.5	7	12	5.5	46.2	0.6	2.7	79.4	0.7	0.6	8.1	4.2	8.9	66.5
JnS2S7	7	145.2	319.7	9.2	23.3	10	4.6	6.7	1.7	8.8	9.6	5.9	48.4	0	3.3	84.3	1.2	1.4	9.9	4.9	10	87.9
JnS2S8	8	169.4	315.4	8.6	24.5	17.3	4.2	6	1.5	8.1	12.9	6.3	46.8	0	2.9	85.3	1.5	1.3	10.6	5.1	11.9	83.9
JnS2S9	9	193.6	319	9.3	43.1	21.6	4.7	5.6	1.7	8.8	16.4	6.8	47.9	0.8	3.1	86	2.1	1.6	9.1	5.2	12.4	115.6
JnS2S10	10	217.8	317.6	12.5	16.2	6.5	4.8	7.6	2.2	9.3	6.1	6.7	49	1.2	3.3	88.4	1.8	1.5	11.4	5.5	12.9	145.5
JnM1S1	1	0	345	17	14	4	5	6	3	11	7	7	57	1	3	43	3	2	12	7	14	139
JnM1S1A	1	0	324	32	24	2	6	12	5	17	10	10	58	2	4	51	6	3	16	12	21	346
JnM1S1B	1	0	306	19	16	2	6	11	3	12	9	8	52	1	4	48	3	2	11	8	15	179
JnM1S2	2	76	258	19	19	15	6	9	4	12	8	7	44	1	4	38	3	2	14	8	17	200
JnM1S3	3	152	226	17	17	6	5	9	3	14	10	6	39	1	3	34	3	2	15	7	22	174
JnM1S3A	3	152	290	20	27	12	6	10	4	14	9	8	51	2	4	44	3	2	14	9	18	240
JnM1S3B	3	152	250	18	20	6	5	8	3	15	10	6	44	1	4	38	3	2	16	8	22	207
JnM1S4	4	228	162	6	10	6	5	6	2	10	7	4	27	0	4	23	1	1	9	5	14	85
JnM1S4B	4	228	256	18	28	8	5	9	4	11	7	7	46	3	3	53	4	2	17	9	15	279
JnM1S5	5	304	169	6	6	6	3	4	1	5	5	3	26	2	3	30	0	0	10	4	11	42
JnM1S5A	5	304	291	22	21	5	6	11	4	15	9	8	51	2	4	44	4	2	19	10	18	241
JnM1S6	6	380	158	3	7	5	4	5	1	8	8	3	24	0	4	22	1	1	7	3	9	38
JnM1S6B	6	380	238	16	18	6	5	9	3	11	9	7	41	2	3	41	3	2	14	8	15	189
JnM1S7	7	456	195	14	14	12	4	8	2	11	8	6	32	2	3	30	2	2	11	6	13	129
JnM1S8	8	532	177	6	8	1	4	6	2	8	7	4	28	1	3	23	0	1	9	4	10	68
JnM1S8A	8	532	180	7	13	22	4	6	2	11	9	5	29	1	3	23	2	1	10	5	12	73
JnM1S9	9	608	189	10	10	27	4	6	2	10	7	4	30	1	4	24	1	1	10	5	12	92
JnM1S10	10	684	211	9	12	4	5	6	2	10	7	4	34	1	3	27	2	1	11	6	11	129
JnM2S1	1.00	0.00	185	3	32	72	3	5	1	8	12	3	26	0	3	19	0	1	7	3	43	39
JnM2S3	3.00	82.50	238	13	20	18	4	9	2	11	9	5	34	2	3	37	2	1	20	6	23	102
JnM2S3	3.00	165.00	187	6	146	123	4	6	1	10	55	4	28	0	3	23	1	1	11	4	81	62
JnM2S4	4.00	247.50	208	10	18	25	4	7	2	8	10	5	33	2	2	30	1	1	15	7	25	65
JnM2S5	5.00	330.00	217	9	16	9	4	6	2	9	11	5	35	2	3	30	2	2	15	6	14	78
JnM2S6	6.00	412.50	241	9	37	17	4	4	2	10	17	5	37	1	3	30	1	1	14	5	12	53
JnM2S7	7.00	495.00	238	5	60	41	4	6	1	8	29	4	36	2	3	28	1	1	12	5	12	50
JnM2S8	8.00	577.50	286	11	14	4	5	8	2	11	9	5	44	1	3	33	1	1	14	6	15	75
JnM2S9	9.00	660.00	246	6	12	3	4	7	1	8	6	4	35	1	3	26	1	1	11	4	10	45
JnM2S10	10.00	742.50	235	9	132	34	4	6	2	9	41	5	36	2	3	29	1	1	14	5	13	60
JnL1S1	1	0	260.1	4.4	7.5	5.4	3.5	4.6	1.1	5.4	5.1	8.9	45.6	0.7	2.7	82.9	0.8	1.1	6.8	2.4	8.8	48.1
JnL1S2	2	216	358.1	9.8	9.5	4	3.6	4.3	1.4	7	6	9.8	44.2	1.8	2.9	94.9	1.6	1.4	8.2	3.5	20.8	104
JnL1S3	3	432	286.3	11.6	11	3.2	4.1	4	1.5	9.1	6	11.3	49.4	0.4	3.2	105.1	2.2	1.9	8.3	3.6	18.5	118.2
JnL1S4	4	648	302.5	3.8	35.8	20.3	3.6	3.6	1	5.2	16	7.3	44.7	0.1	3	75.4	1	1	4.7	2.5	9.1	32.2
JnL1S5	5	864	392.5	3.5	9.8	4.2	3.4	3.4	0.7	6.2	7	6	37	0	2.8	64.4	0.7	1	5	1.9	7.1	24.2
JnL1S6	6	1080	321	2.5	58.3	24.2	3.8	4	0.9	6.8	23.7	6.9	42.4	0	2.9	74.7	0.4	0.6	4.7	2.4	8.4	33.3
JnL1S7	7	1296	274.4	7.9	7.1	5	3.8	4.1	0.8	7.1	7.5	6.5	42	0	3.1	73.8	0	0.5	5.1	2.3	7.3	31.2
JnL1S8	8	1512	284.7	7.2	9.2	3.5	4.1	3.2	0.9	7.4	6.3	8	46.8	0	2.8	78.7	0.4	0.9	6.4	2.4	9.5	49.7
JnL1S9	9	1728	296.6	9.5	14.6	3.6	4.1	5.4	1.7	7.4	6.1	11.4	53.5	0.6	2.7	101.4	2.5	1.9	8.5	3.9	14.1	150
JnL1S10	10	1944	339.7	5.8	9.3	5.8	4.4	5.7	1.1	6.1	7.1	9.6	48.8	0.2	2.7	85.8	1.1	1.1	7.3	3	12.1	64.3
JnL2S1	1	0	170.4	6.6	7.4	3	3.4	2.1	1.1	8.2	6.8	2.8	21.7	0.5	2.9	58.5	0.8	0.7	6.7	3.3	15.4	73
JnL2S2	2	159.6	142.3	1.7	8.6	9.8	3	3.1	0.9	5.9	8.9	2.1	17.7	0.9	2.7	45.8	0.2	0.5	6	2.6	16.8	46.6
JnL2S3	3	319.2	996.1	0	20.9	19.3	2.2	3.1	0.7	7.1	14.8	1	9.5	0.8	2.9	44.5	0.4	0.5	7.8	2.4	13.3	31.6
JnL2S4	4	478.8	114.2	2.4	18.2	14.6	2.5	2.8	0.8	7	12.8	1.7	14.4	0.9	2.6	48.1	0.3	0.4	6.2	2.6	11.5	34
JnL2S5	5	638.4	195.2	0.2	10.9	8.2	2.5	4.5	0.6	7.5	9.1	2.2	16.3	0.3	2.9	48.9	0.1	0.3	5.4	2.1	8.8	27.2
JnL2S6	6	798	249.8	2.7	22	16.6	3.3	2.9	0.8	6.6	13.2	3.3	26.6	0	2.6	59.6	0.8	0.9	5.7	2.2	8.2	33.6
JnL2S7	7	957.6	213.5	2.7	35.7	16.5	3.6	2.2	0.9	7.5	17.6	3.8	27.1	0	3	54	0.2	0.4	4.3	2.3	8.2	32
JnL2S8	8	1117.2	196	4.8	15.2	9.6	3.4	6.9	1.3	7.9	10.1	3.7	26.2	0	2.8	70.3	1.5	1	6.2	3	10.2	74.8
JnL2S9	9	1276.8	286.1	12.1	11.7	6.4	4.4	7.2	2.2	6.9	7.6	6.7	42.5	1.6	2.5	111.3	2.2	1.8	11.8	5.2	17.5	133.7
JnL2S10	10	1436.4	288.8	9.7	11.4	5.3	4.6	5.5	1.8	8.5	6.9	6.2	41.9	1.1	3	102.1	1.7	1.2	8.4	4.3	12.6	105.8
		Average Concentration	301.92	9.20	23.64	14.39	4.15	5.98	1.78	8.90	11.35	5.65	38.33	0.96	3.06	57.27	1.48	1.21	9.98	4.82	15.14	98.04

Coral Pink Sand Dunes Major Element XRF Data												
Sample Name	Sample Position	Foreset Length (inches)	Major Elements - Concentration in Weight Percent									
			SiO2	TiO2	Al2O3	Fe2O3	MnO	MgO	CaO	Na2O	K2O	P2O5
CPS1S1	1	0	97.098	0.01	1.295	0.167	0.001	0	0	0	0.842	0.013
CPS1S2	2	12	97.239	0.012	1.254	0.159	0.002	0.002	0	0	0.809	0.011
CPS1S3	3	24	96.931	0.021	1.341	0.164	0.002	0	0	0.082	0.882	0.012
CPS1S4	4	36	96.992	0.02	1.356	0.165	0.002	0	0	0	0.891	0.011
CPS1S5	5	48	96.949	0.012	1.425	0.195	0.002	0.012	0.002	0	0.906	0.013
CPS1S6	6	60	96.752	0.022	1.449	0.185	0.002	0.008	0	0	0.941	0.013
CPS1S7	7	72	96.656	0.027	1.51	0.175	0.001	0.022	0	0	0.955	0.012
CPS1S8	8	84	96.43	0.02	1.562	0.178	0.002	0.004	0	0	1.006	0.012
CPS1S9	9	96	96.603	0.027	1.603	0.188	0.002	0.011	0	0	1.043	0.012
CPS1S10	10	108	97.059	0.021	1.355	0.162	0.002	0.012	0	0	0.814	0.012
CPS2S1	1	0	99.071	0	0.463	0.102	0.001	0	0	0	0.229	0.008
CPS2S1.5	1.5	28	98.901	0.003	0.491	0.103	0	0	0	0	0.247	0.007
CPS2S2	2	56	98.812	0	0.573	0.112	0.001	0	0	0	0.296	0.007
CPS2S3	3	112	98.263	0	0.769	0.126	0.001	0	0	0	0.451	0.007
CPS2S4	4	168	97.883	0	0.899	0.137	0.001	0	0	0	0.545	0.008
CPS2S5	5	224	97.557	0.002	1.004	0.15	0.001	0	0	0	0.629	0.009
CPS2S6	6	280	97.872	0	0.894	0.142	0.001	0	0	0	0.547	0.008
CPS2S7	7	336	97.75	0.009	0.968	0.151	0.002	0	0	0	0.609	0.007
CPS2S8	8	392	97.079	0.001	1.349	0.188	0.002	0.01	0	0	0.909	0.01
CPS2S9	9	448	96.69	0.032	1.447	0.21	0.002	0.002	0	0	0.973	0.011
CPS2S10	10	504	97.588	0	1.098	0.16	0.001	0	0	0	0.7	0.009
CPM1S1	1	0	98.367	0	0.754	0.131	0.001	0	0	0	0.429	0.01
CPM1S2	2	85	97.814	0.015	0.988	0.148	0.001	0	0	0	0.602	0.009
CPM1S3	3	170	97.549	0.021	1.065	0.158	0.002	0.003	0	0	0.655	0.01
CPM1S4	4	255	97.497	0.013	1.155	0.158	0.002	0	0	0	0.721	0.011
CPM1S5	5	340	97.674	0.011	1.186	0.162	0.002	0	0	0	0.747	0.011
CPM1S6	6	425	96.971	0.03	1.328	0.18	0.002	0.008	0	0	0.86	0.011
CPM1S7	7	510	97.331	0.026	1.222	0.165	0.002	0	0	0	0.785	0.011
CPM1S8	8	595	97.235	0.016	1.162	0.165	0.002	0.002	0	0	0.733	0.011
CPM1S9	9	680	97.256	0.018	1.195	0.162	0.002	0	0	0	0.761	0.011
CPM1S10	10	765	97.163	0.027	1.102	0.171	0.002	0	0	0	0.681	0.011
CPM2S1	1	0	97.958	0.006	0.957	0.147	0.001	0	0	0	0.582	0.01
CPM2S2	2	94	98.419	0	0.783	0.142	0.001	0	0	0	0.462	0.01
CPM2S3	3	188	98.695	0.01	0.574	0.111	0.001	0	0	0	0.314	0.008
CPM2S4	4	282	98.767	0	0.606	0.113	0	0	0	0	0.323	0.01
CPM2S5	5	376	98.372	0.016	0.76	0.135	0.001	0	0	0	0.426	0.011
CPM2S6	6	470	98.271	0.007	0.819	0.136	0.001	0	0	0	0.479	0.01
CPM2S7	7	564	97.863	0.013	1.064	0.155	0.001	0.003	0	0	0.662	0.011
CPM2S8	8	658	98.119	0.008	0.913	0.144	0.001	0	0	0	0.554	0.01
CPM2S9	9	752	98.154	0.014	0.835	0.143	0.001	0.004	0	0	0.493	0.01
CPM2S10	10	846	97.105	0.024	1.323	0.174	0.002	0.007	0	0	0.861	0.012
CPL1S1	1	0	98.036	0.012	0.933	0.153	0.002	0	0	0	0.587	0.009
CPL1S2	2	209	98.34	0.015	0.759	0.133	0.001	0	0	0	0.439	0.009
CPL1S3	3	418	98.351	0.012	0.775	0.13	0.001	0	0	0	0.458	0.009
CPL1S4	4	627	98.295	0	0.866	0.137	0.002	0	0	0	0.518	0.01
CPL1S5	5	836	97.887	0.011	0.928	0.138	0.001	0	0	0	0.571	0.01
CPL1S6	6	1045	97.994	0.013	0.98	0.149	0.002	0	0	0	0.609	0.011
CPL1S7	7	1254	97.849	0.019	0.971	0.143	0.001	0	0	0	0.598	0.01
CPL1S8	8	1463	97.384	0.018	1.293	0.17	0.002	0.053	0	0	0.851	0.011
CPL1S9	9	1672	98.156	0.006	0.897	0.139	0.001	0	0	0	0.543	0.01
CPL1S10	10	1881	97.994	0.014	1.012	0.144	0.001	0	0	0	0.638	0.01
CPL2S1	1	0.00	98.66	0.01	0.61	0.17	0.00	0.01	0.02	0.00	0.31	0.01
CPL2S2	2	160.00	97.73	0.01	0.93	0.16	0.00	0.00	0.00	0.00	0.56	0.01
CPL2S3	3	320.00	98.07	0.01	0.98	0.14	0.00	0.00	0.00	0.00	0.61	0.01
CPL2S4	4	480.00	97.87	0.02	1.02	0.15	0.00	0.00	0.00	0.00	0.64	0.01
CPL2S5	5	640.00	97.78	0.01	1.02	0.15	0.00	0.00	0.00	0.00	0.64	0.01
CPL2S6	6	800.00	97.03	0.02	1.46	0.17	0.00	0.00	0.00	0.00	0.97	0.01
CPL2S7	7	960.00	96.94	0.04	1.41	0.19	0.00	0.00	0.00	0.00	0.93	0.01
CPL2S8	8	1120.00	97.27	0.02	1.21	0.17	0.00	0.00	0.00	0.00	0.78	0.01
CPL2S9	9	1280.00	96.48	0.04	1.57	0.21	0.00	0.00	0.00	0.00	1.08	0.01
CPL2S10	10	1440.00	97.25	0.03	1.18	0.17	0.00	0.00	0.00	0.00	0.75	0.01
		Average Concentration	97.67	0.01	1.06	0.15	0.00	0.00	0.00	0.00	0.66	0.01

Coral Pink Sand Dunes Trace Element XRF Data																						
Sample Name	Sample Position	Foreset Length (inches)	Trace Elements - Concentration in Parts Per Million																			
			Ba	Ce	Cr	Cu	Ga	La	Nb	Nd	Ni	Pb	Rb	Sc	Sm	Sr	Th	U	V	Y	Zn	Zr
CPS1S1	1	0	154	1.8	2.5	0.8	2.6	4.1	0.6	6.8	4.9	2.9	21.2	0	2.7	15.6	0.1	0.3	3.3	1.7	4	20.4
CPS1S2	2	12	144.3	0	2.6	0.2	2.4	3.4	0.4	7.2	4.6	2.6	20	0	2.9	15.1	0.4	0.4	3.3	1.5	3.6	19.8
CPS1S3	3	24	156.3	1.9	2.6	0	2.6	3.4	0.4	9	5.1	2.8	22.1	0	2.8	16.3	0.1	0.4	3.4	1.8	3.8	21.7
CPS1S4	4	36	161	1.1	4	0	2.6	4	0.6	6.9	5.5	3.5	22.8	0	2.7	17	0.1	0.4	3.6	1.7	3.6	21.2
CPS1S5	5	48	159.2	4	3.3	0.6	2.3	2.8	0.7	5.7	4.6	3.2	22.1	0	2.9	16.5	0.2	0.4	3.7	1.5	4.4	19.7
CPS1S6	6	60	155.6	0.7	2.7	0	2.7	4.1	0.5	6.3	3.9	2.4	20.9	0	2.7	15.7	0	0.4	3.1	1.7	3.7	23.2
CPS1S7	7	72	147.6	0.9	3.1	0.1	2.3	4.1	0.5	5.1	3.4	2.5	20.8	0	2.1	15.7	0	0.2	4	1.4	4	21.9
CPS1S8	8	84	145.3	2.3	3.1	0	2.2	2.3	0.6	6	3.4	3.1	20.8	0	2.5	15.5	0.2	0.6	4.1	1.4	3.7	23
CPS1S9	9	96	143.4	2.8	2.4	0.5	2	3.6	0.5	4.1	3.5	3.2	21.8	0	2.4	15.5	0	0.3	4	1.5	3.9	32.3
CPS1S10	10	108	126.6	0	3.4	0.2	2	2.4	0.5	4.6	3	2.4	17.6	0	2.5	12.9	0.3	0.4	4.1	1.4	3.4	20.4
CPS2S1	1	0	46.5	0.5	2.4	0	1.9	1.8	0.3	7.9	4.4	1.2	7	0	2.8	5.2	0	0.3	2.1	1.5	2.2	18.8
CPS2S1.5	1.5	28	48.8	1.3	2.4	0	1.8	2.9	0.5	7	4.2	0.4	7.3	0	3.1	5.5	0	0.1	2	1.4	2.7	19.9
CPS2S2	2	56	62.3	0	2.8	0	2.2	2.2	0.5	9.8	4.8	1.4	8.6	0	3.3	6.8	0.6	0.4	3.3	1.4	2.9	18.7
CPS2S3	3	112	90.1	0.3	3.3	0	2.2	2.4	0.5	8.5	5.5	1.7	12.1	0	3.1	9.2	0	0	3	1.4	2.8	19
CPS2S4	4	168	100.8	0.8	3	0	2.3	2.5	0.5	7.7	4.7	1.8	13.7	0	2.8	10.7	0.2	0.5	2.3	1.3	3	18.8
CPS2S5	5	224	109	3.4	2.3	0	2.5	4.1	0.6	8.4	4.3	2.5	15.3	0	2.9	11.6	0.5	0.5	3.3	1.6	3.6	30.6
CPS2S6	6	280	97.5	0	3.6	0	2.1	1.7	0.4	8.6	5.2	1.5	13.9	0	3.6	10.1	0	0.2	2.3	1.5	3.1	25.6
CPS2S7	7	336	104.1	1.2	4	0	2.3	2.9	0.6	8.1	5.3	2	15.2	0	3.1	11.3	0.4	0.4	3.7	1.8	3.4	39
CPS2S8	8	392	135.7	3.9	6.1	0	2.3	3.1	0.7	6.6	5.3	2.7	20.8	0	3.2	14.6	0	0.4	2.5	1.9	3.8	47
CPS2S9	9	448	149	2.3	8.5	0	2.3	2.6	0.6	6.8	4.7	3.4	22.4	0	3	15.6	1.1	0.9	4.2	2.5	4.1	82
CPS2S10	10	504	122.3	4.7	4.5	0	2.3	3.8	0.6	7.2	4.5	1.7	16.7	0	2.9	13	0	0.3	2.8	1.6	3.5	40.5
CPM1S1	1	0	86.7	0.5	2.8	0.1	2	1.6	0.5	7.1	4.4	1.2	11.6	0	2.6	9.3	0	0.1	2.5	1.2	3.4	18.5
CPM1S2	2	85	111.4	0	2.4	0	2.7	1.7	0.4	7.9	5.1	2.6	15.6	0	3	12.1	0.2	0.5	2.6	1.8	3.8	23.5
CPM1S3	3	170	120.3	0.7	2.7	0	2.4	1.3	0.5	7.1	5.1	1.6	16.7	0	2.8	12.7	0	0.1	3	1.6	3.8	37.1
CPM1S4	4	255	122.7	2.9	3.9	0	2.3	1.5	0.6	7	4.1	2.3	17.5	0	2.8	14	0	0.3	3.7	1.6	3.9	21.9
CPM1S5	5	340	137	3.3	2.9	0	2.5	3.7	0.4	7.5	3.9	2.3	18	0	3	13.6	0.3	0.7	3.3	1.6	3.8	25.4
CPM1S6	6	425	154.9	0.2	4.3	0	3.1	1.5	0.7	7.4	5.1	2.9	22.3	0	2.7	16	0.3	0.4	1.7	1.8	4.2	42.4
CPM1S7	7	510	140.3	1.6	2.2	0	2.7	1.4	0.7	7.5	5.3	2.7	20.2	0	3.2	15.9	0	0.3	2.4	1.6	4.2	31.1
CPM1S8	8	595	140.2	3	3.9	0	3	3.1	0.5	9	5.7	2.7	19.2	0	3	14.3	0	0.2	3.2	1.6	4.2	30.2
CPM1S9	9	680	138.3	1.3	3.8	0	2.7	3.4	0.6	7.4	4.7	2.3	18.9	0	2.9	14	0.2	0.5	3.1	1.6	4.5	27.8
CPM1S10	10	765	120.8	3.5	3.9	0	2.6	4.9	0.5	7.6	5.5	2.1	17.5	0	3.4	13.7	0.1	0.3	3.3	1.6	4	33.4
CPM2S1	1	0	99.3	4.6	2.6	0	2.2	2.7	0.6	6.7	4.1	1.6	14.5	0	2.8	11	0	0.4	2.8	1.7	3.4	26.8
CPM2S2	2	94	77.8	0	2.3	0	2.1	2.8	0.5	7.2	3.8	1.2	11	0	2.8	7.9	0	0.2	1.7	1.3	3.2	24.2
CPM2S3	3	188	59	0	2.4	0	2.6	2.6	0.6	7.5	5	0.9	9	0	3.2	6.3	0.4	0.5	1.7	1.6	2.6	23.7
CPM2S4	4	282	65.5	0	1.8	0	2.3	3.7	0.4	7.2	4.4	0.9	8.6	0	2.9	6.4	0.1	0.3	3.1	1.2	2.9	17.8
CPM2S5	5	376	87.8	0.8	2	0	2.7	0.9	0.4	7.8	4.6	1.4	12	0	3.3	9.6	0	0.2	3.5	1.4	3.3	19.5
CPM2S6	6	470	92.9	0	2.4	0	2.5	2.8	0.4	7.7	5	1	12.8	0	3.3	9.9	0	0.1	2.8	1.5	3.2	19
CPM2S7	7	564	116.3	0	4	0	2.5	3.8	0.5	7.1	4.5	2.5	16.9	0	3.1	12.5	0.2	0.5	3.2	1.5	3.7	25.6
CPM2S8	8	658	95.6	0.1	3	0	2.4	3.4	0.5	8.4	4.3	1.6	13.7	0	2.8	10.5	0	0.2	2.6	1.4	3.3	26.3
CPM2S9	9	752	88.5	0.7	2.5	0	2.4	4.1	0.5	7.1	4.7	1.5	12.6	0	3	9.3	0.4	0.7	4.1	1.7	3.4	41.1
CPM2S10	10	846	148.6	1.1	7.6	0	2.9	2.6	0.8	9	5.9	3.5	21.7	0	2.8	15.5	0.6	0.9	3.3	2	4	36.1
CPL1S1	1	0	100	1	2.5	0	2.5	2.6	0.6	8.2	5.1	2.1	14.9	0	2.9	11.1	0	0.3	2.7	1.6	3.4	36.5
CPL1S2	2	209	82.6	0	2.2	0	2.4	1.5	0.5	6.8	4.1	1.2	11.7	0	2.7	8.8	0	0	2.4	1.5	3.9	33.1
CPL1S3	3	418	85.8	0	1.8	0	2.1	3.5	0.6	8.1	5.1	1.5	11.9	0	2.9	9	0	0.2	2	1.6	3.1	21.3
CPL1S4	4	627	92.8	0	3.7	0	2.5	3.5	0.5	6.6	5.6	1.5	13.6	0	3.2	10.3	0	0.1	2.5	1.6	3.4	25.7
CPL1S5	5	836	107.9	0.6	2.7	0	2.4	2	0.8	8.1	5.1	1.3	14.6	0	3.1	11.1	0	0.1	3.4	1.5	3.7	25.2
CPL1S6	6	1045	102.6	0.7	3.1	0	2.3	2	0.6	7.4	4.5	1.7	14.4	0	3.1	10.7	0	0.1	3.5	1.5	3.3	23.7
CPL1S7	7	1254	108.6	0	3	0	2.8	2	0.7	7.1	5.5	1.8	15.5	0	3.5	11.6	0	0.1	2.7	1.6	3.9	23.3
CPL1S8	8	1463	132.4	0	4.1	0	2.4	2.4	0.4	7.6	4.8	3	19.7	0	2.8	14.3	0.5	0.7	3.3	1.6	3.8	29.8
CPL1S9	9	1672	91.8	0	2.8	0	1.8	1.5	0.5	7.2	5	1.5	13.2	0	3.2	10	0.1	0.3	3.5	1.6	3.4	20.9
CPL1S10	10	1881	103.1	0	2.8	0.3	2.1	3.2	0.3	7.1	4.4	1.7	14.7	0	2.7	10.3	0.6	0.6	2.9	1.7	3.4	26.4
CPL2S1	1	0.00	60	2	4	1	2	1	1	8	5	1	9	0	3	8	0	0	5	2	4	27
CPL2S2	2	160.00	108	0	2	0	3	3	1	8	5	2	15	0	3	12	0	0	3	2	4	21
CPL2S3	3	320.00	110	0	2	0	2	3	1	8	5	2	16	0	3	12	0	0	4	1	4	20
CPL2S4	4	480.00	117	3	2	0	3	2	1	8	5	2	16	0	3	12	0	0	2	2	3	20
CPL2S5	5	640.00	116	0	3	0	3	3	1	9	5	2	17	0	3	12	0	1	1	2	4	29
CPL2S6	6	800.00	164	1	2	0	3	4	1	8	5	3	23	0	3	17	0	0	3	2	4	24
CPL2S7	7	960.00	153	1	3	0	3	3	1	7	5	3	23	0	3	17	0	1	3	2	4	56
CPL2S8	8	1120.00	136	2	4	0	3	3	1	7	5	2	20	0	3	15	0	0	4	2	4	42
CPL2S9	9	1280.00	167	4	6	0	3	3	1	7	5	4	26	0	3	18	1	1	3	2	4	81
CPL2S10	10	1440.00	133	5	4	0	3	3	1	9	5	3	19	0	3	14	0	0	3	2	4	43
		Average Concentration	115.33	1.29	3.22	0.06	2.46	2.79	0.61	7.42	4.74	2.11	16.42	0.00	2.94	12.26	0.15	0.34	3.04	1.63	3.61	28.91

Appendix B: Additional PCA Figures

Plots of the first two principal components of XRF data.

First Two Principal Component Plots for All Elements

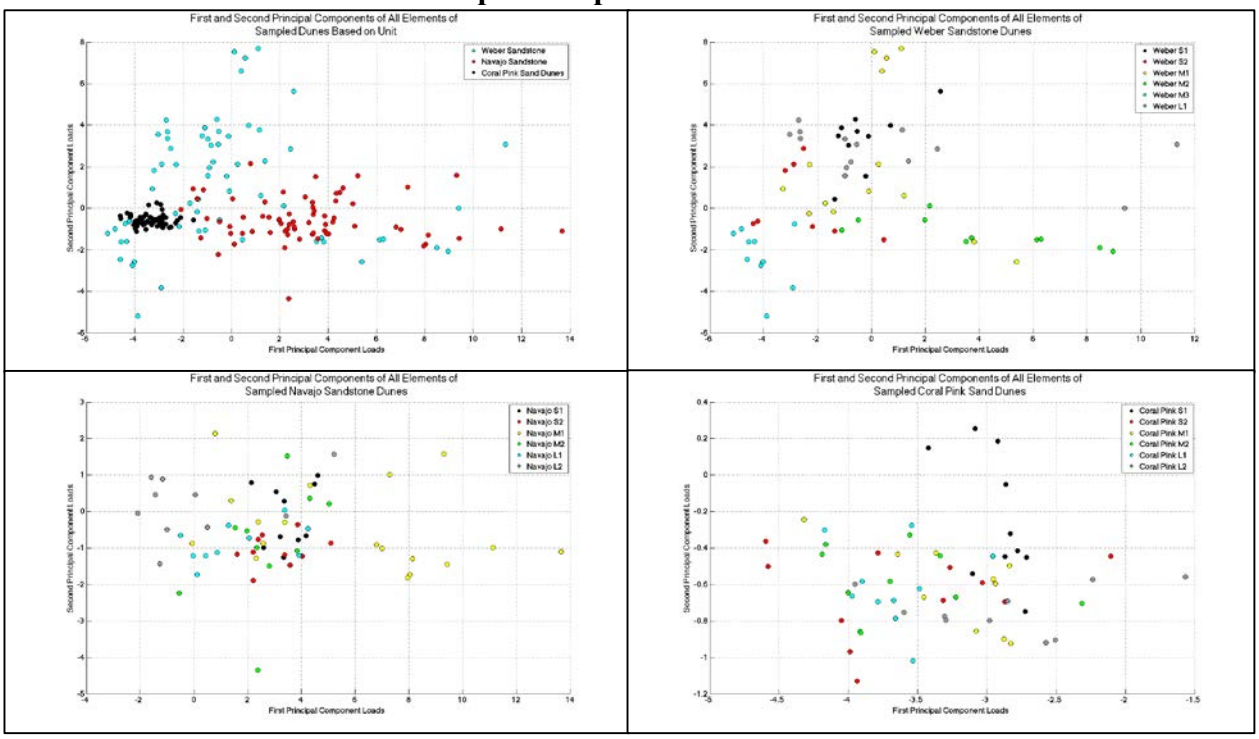

First two principal components of all XRF data for; A – all units, B – Weber Sandstone, C – Navajo Sandstone, and D – Coral Pink Sand Dunes.

First Two Principal Component Plots for Major Elements

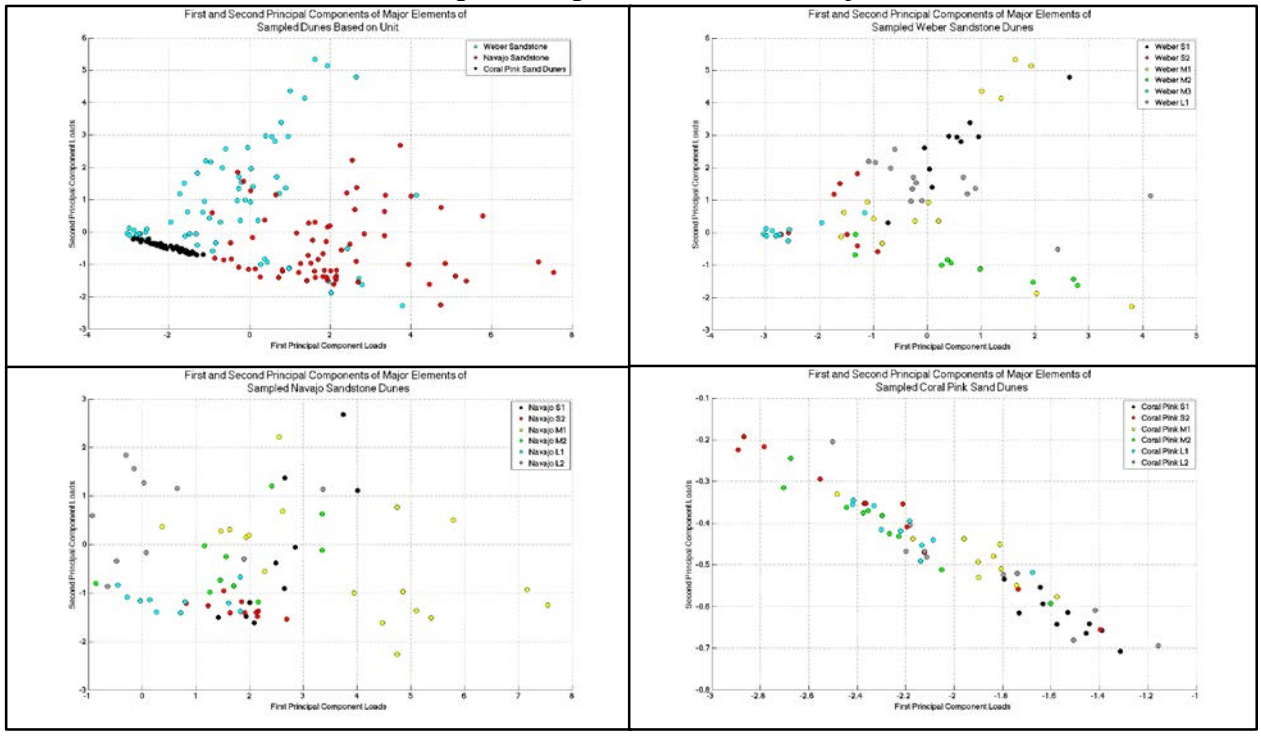

First two principal components of major element XRF data for; A – all units, B – Weber Sandstone, C – Navajo Sandstone, and D – Coral Pink Sand Dunes.

First Two Principal Component Plots for Trace Elements

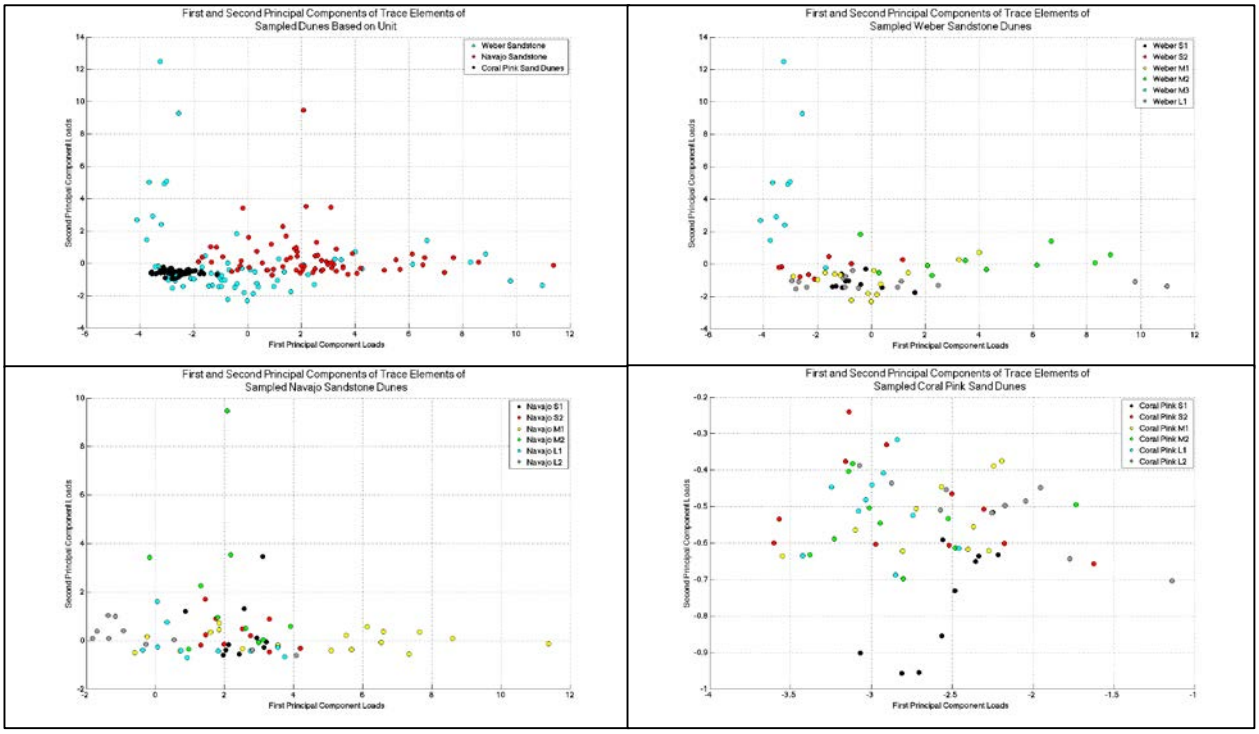

First two principal components of trace element XRF data for; A – all units, B – Weber Sandstone, C – Navajo Sandstone, and D – Coral Pink Sand Dunes.

Appendix C: Core Plug Porosity and Permeability

Some of the samples collected were core plugs of good enough quality to collect porosity and permeability data. Porosity data was collected using a Temco/CLI Ultrapore 300^{TM}, and permeability was measured using a Temco/CLI Ultra Perm 500^{TM} at the Brigham Young University Sedimentology Laboratory according to standard laboratory practices.

Core Plug Porosity		
Unit	Sample Name	Porosity (%)
Navajo Sandstone	JnM1S1	18.6
	JnM1S1A	13.8
	JnM1S2	19.4
	JnM1S3A	19.9
	JnM1S4	17.9
	JnM1S5A	16.6
	JnM1S7	20.1
	JnM1S8A	18.8
	JnM1S9	19.0
Weber Sandstone	PPwL1S1	20.3
	PPwL1S2	21.9
	PPwL1S3	17.7
	PPwL1S4A	17.2
	PPwL1S5A	16.0
	PPwL1S6	16.6
	PPwL1S7	18.5
	PPwL1S8	18.2
	PPwL1S8A	17.8
	PPwL1S9	18.1
	PPwL1S10	22.5
	PPwM1S2	17.4
	PPwM1S3	17.1
	PPwM1S5	16.8
	PPwM1S7	12.7
	PPwM1S8	15.6
	PPwM1S9	16.8
	PPwM1S10	14.8
	PPwS1S1	17.2
	PPwS1S2	17.7
	PPwS1S3B	14.9
	PPwS1S4	15.6
	PPwS1S5	14.1
	PPwS1S6	13.4
	PPwS1S7	19.1
	PPwS1S8 Inner	14.1
	PPwS1S9	14.8
	PPwS1S9A	15.9
	PPwS1S9G	16.5
	PPwS1S10G	15.2
	PPwS2S1	17.1
	PPwS2S2	17.3
	PPwS2S3A	18.4
	PPwS2S4	20.0
	PPwS2S5	21.8
	PPwS2S6	25.2
	PPwS2S7 Inner	20.5
	PPwS2S7 Outer	22.3
	PPwS2S8	20.3
	PPwS2S8A	21.5
	PPwS2S9	22.2
	PPwS2S10 Inner	19.1
	PPwS2S10 Outer	20.0
	PPwM2S1A	15.9
	PPwM2S2B	16.7
	PPwM2S4	19.3
	PPwM2S5	16.8
	PPwM2S7	16.8
	PPwM2S8A	16.6
	PPwM2S9A	16.8
	PPwM2S10A	17.6

Core Plug Permeability		
Unit	Sample Name	Permeability (mD at 500 psi)
Navajo Sandstone	JnM1S1	10.4
	Jn M1 S2	10.6
	Jn M1 S3A	5.9
	Jn M1 S5A	21.8
	Jn M1 S7	111.0
	Jn M1 S8A	33.8
	Jn M1 S9	31.8
Weber Sandstone	PPw L1 S1	5.1
	PPw L1 S2	30.2
	PPw L1 S3	49.1
	PPwS2S1	19.0
	PPwS2S2	22.1
	PPwS2S3A	220.5
	PPwS2S4	303.5
	PPwS2S5	83.4
	PPwS2S6	86.0
	PPwS2S7 Inner	51.2
	PPwS2S7 Outer	57.4
	PPwS2S8A	23.5
	PPwS2S9	138.0
	PPwS2S10 Inner	34.6
	PPwS2S10 Outer	32.4
	PPw L1 S1	5.1
	PPw L1 S2	30.2
	PPw L1 S3	49.1
	PPw L1 S5A	14.8
	PPw L1 S6	33.1
	PPw L1 S7	15.9
	PPw L1 S8	61.9
	PPw L1 S8A	10.9
	PPw L1 S9	78.8
	PPw L1 S10	79.6
	PPw M1 S2	10.3
	PPw M1 S3	5.3
	PPw M1 S5	22.1
	PPw M1 S7	7.0
	PPw M1 S9	23.3
	PPw M1 S10	4.9

Appendix D: Coral Pink Sand Dunes Grain Size Data

Select samples from the Coral Pink L1 dune were analyzed for grain size data.

Sample:	CP L2 S1
Tray Weight:	1.3170
Sample Weight:	38.1784

Mesh Size			Mass sample and tray (g)	Mass tray (g)	Mass Sample (g)	Mass %
Phi	µm	inches				
No 25	710	0.0278	1.3347	1.3339	0.0008	2.09543E-05
No 35	500	0.0197	1.6013	1.2795	0.3218	0.00842885
No 45	355	0.0139	16.1138	1.3042	14.8096	0.387905203
No 60	250	0.0098	16.6058	1.3108	15.295	0.400619198
No 80	180	0.007	7.445	1.3362	6.1088	0.160006705
No 120	125	0.0049	2.5692	1.3159	1.2533	0.032827463
No 170	90	0.0035	1.4205	1.2745	0.146	0.003824152
No 230	63	0.0025	1.337	1.309	0.028	0.000733399
No 325	45	0.0017	1.2954	1.2919	0.0035	9.16749E-05
Finer than 325	<45	<0.0017	1.3085	1.2999	0.0086	0.000225258
				Totals	37.9754	0.994682857

Sample:	CP L2 S4
Tray and Sample Weight:	39.8151
Tray Weight:	1.2746
Sample Weight:	38.5405

Mesh Size			Mass sample and tray (g)	Mass tray (g)	Mass Sample (g)	Mass %
Phi	µm	inches				
No 25	710	0.0278	0	0	0	0
No 35	500	0.0197	1.3264	1.323	0.0034	8.82189E-05
No 45	355	0.0139	1.393	1.3373	0.0557	0.001445233
No 60	250	0.0098	14.69	1.3358	13.3542	0.34649784
No 80	180	0.007	22.7314	1.3241	21.4073	0.555449462
No 120	125	0.0049	4.9456	1.279	3.6666	0.095136285
No 170	90	0.0035	1.4306	1.3156	0.115	0.002983874
No 230	63	0.0025	1.3213	1.3123	0.009	0.000233521
No 325	45	0.0017	0	0	0	0
Finer than 325	<45	<0.0017	0	0	0	0
				Totals	38.6112	1.001834434

Sample:	CP L2 S8
Tray and Sample Weight:	38.5594
Tray Weight:	1.3257
Sample Weight:	37.2337

Mesh Size			Mass sample and tray (g)	Mass tray (g)	Mass Sample (g)	Mass %
Phi	µm	inches				
No 25	710	0.0278	0	0	0	0
No 35	500	0.0197	1.322	1.3205	0.0015	4.02861E-05
No 45	355	0.0139	1.7881	1.3137	0.4744	0.012741146
No 60	250	0.0098	12.1781	1.3162	10.8619	0.291722284
No 80	180	0.007	18.058	1.3197	16.7383	0.44954705
No 120	125	0.0049	9.3747	1.2984	8.0763	0.216908338
No 170	90	0.0035	2.142	1.3306	0.8114	0.021792086
No 230	63	0.0025	1.5254	1.3218	0.2036	0.005468165
No 325	45	0.0017	1.3742	1.3298	0.0444	0.001192468
Finer than 325	<45	<0.0017	1.336	1.3224	0.0136	0.000365261
				Totals	37.2254	0.999777084

Sample:	CP L2 S10
Tray and Sample Weight:	42.3658
Tray Weight:	1.3221
Sample Weight:	41.0437

Mesh Size			Mass sample and tray (g)	Mass tray (g)	Mass Sample (g)	Mass %
Phi	µm	inches				
No 25	710	0.0278	0	0	0	0
No 35	500	0.0197	1.3147	1.314	0.0007	1.7055E-05
No 45	355	0.0139	1.4194	1.3202	0.0992	0.002416936
No 60	250	0.0098	13.6408	1.3339	12.3069	0.299848698
No 80	180	0.007	23.0763	1.3361	21.7402	0.529684215
No 120	125	0.0049	6.4717	1.2738	5.1979	0.126643066
No 170	90	0.0035	2.4802	1.3158	1.1644	0.028369762
No 230	63	0.0025	1.777	1.3101	0.4669	0.01137568
No 325	45	0.0017	1.371	1.3258	0.0452	0.001101265
Finer than 325	<45	<0.0017	1.3192	1.3162	0.003	7.30928E-05
				Totals	41.0244	0.999529769